I. N. Meshkov

BARRIER BUCKET METHOD
IN CYCLIC ACCELERATORS

Мешков И. Н.   Д9-2013-53

Метод барьерных напряжений в циклических ускорителях

В статье представлен принцип действия систем барьерного ВЧ-напряжения, которые находят применение для накопления и ускорения заряженных частиц в протонных синхротронах — накопителях. Описание дано на примере двух моделей таких систем — с прямоугольными и квазисинусоидальными барьерами. Используется два различных способа описания динамики частиц в синхротронах с барьерным ВЧ-напряжением. Первый из них — «пошаговый» анализ движения частицы в фазовом пространстве «импульс–фаза», который позволяет дать ясное и простое описание физических принципов метода и получить его главные характеристики в аналитической форме. Этот способ, однако, не всегда эффективен. Поэтому в статье представлен и широко используется способ анализа динамики частиц в барьерных системах с помощью решения дифференциальных уравнений фазового движения. Этот способ позволяет производить как вычисления в аналитической форме, так и численное моделирование, что иллюстрируется приведенными примерами.

Meshkov I. N.   D9-2013-53

Barrier Bucket Method in Cyclic Accelerators

The paper describes the main principles of the Barrier Bucket Method of charge particles stacking and acceleration in proton synchrotrons. The consideration is done with two models of "rectangular barriers" and "quasi-sinusoidal" ones using different approaches to analysis of particle motion. The first of them — so-called "step by step approach", allows us to give a very clear physical explanation of the method and obtain easily the main characteristics of the method in analytical form. However, that is not always an efficient way. Therefore, the general case of the "barriers" of an arbitrary form is considered as well and differential equations of particle phase motion are derived. This approach gives ample opportunities for analysis and numerical simulations of different phase dynamics regimes of particles in cyclic accelerators. Numerical examples for the method illustration are presented.

INTRODUCTION

The Barrier Buckets (BB) method has been proposed in 1983 by J. E. Griffin [1] and since that time was applied to storage and acceleration of particles in proton synchrotrons (e. g. see review article [2]). The idea of the method is based on application of periodic RF voltage pulses synchronous with the particle revolution (e. g., of rectangular form) for storage and/or acceleration charged particles in cyclic accelerators. Such pulses are generated with a broad-band RF system that is constructed with RF cavities loaded with ferrites, amorphous iron and similar RF ferromagnetic materials.

In recent years an interest to application of this method in different projects was reactivated due to development of both stochastic and electron cooling methods. Two projects — Nuclotron-based Ion Collider fAcility (NICA) [3] at Joint Institute for Nuclear Research at Dubna and Facility for Antiproton and Ion Research (FAIR) [4] at Darmstadt plan to construct ion storage rings and colliders, where this method will be used both for stacking and acceleration of ions.

The charged particle dynamics in cyclic accelerators with barrier voltage RF system is described with the equations similar to those for classic RF systems of harmonic voltage [5]. However, some peculiarities of particle dynamics in barrier systems require a special consideration. The methods of numerical simulation developed for this purpose [2, 6–14] are very fruitful and give good results of practical importance. They have been bench-marked persuasively versus experiments without [8] and with [10, 14] cooling applied. Nevertheless, these methods are able to give us answers "yes" or "no", and a lack of analytical approach exists.

This article has a goal to describe the physics principles of the barrier method and different regimes of its application and also to give a set of formulae useful for analytical estimates.

Widely used way of description of BB method is based on a consideration of particle energy variation at interaction with the barrier voltage potential well (see for

instance Ref. 6, 15). More clear explanation of the method principle is based on a consideration of the particle motion in the longitudinal phase space where a RF system generates a sequence of alternate pulses of equal amplitudes V at the equilibrium particle revolution frequency. Then, if a particle somehow is "inserted" into phase interval between phases $\varphi = 0$ and $\varphi = \varphi_s \equiv 2 \cdot \Delta\varphi_B + \varphi_{BB}$ (Fig. 1) its phase trajectory can be stable at certain conditions. These conditions we will find first using in the next Section *the "step by step" approach*. The general case for arbitrary barriers is considered in paragraph Section 2. The procedure of particle insertion (stacking) into the stable phase area is described in Section 3. The particle acceleration with barrier voltage is presented in Section 4. Most sophisticated versions of the method application based on so called moving barriers technique is considered in Section 5. Some technical characteristics of barrier RF systems existed before and developed in recent years are described in Section 6. All numerical examples are given for parameter values, related to the NICA project.

The option of BB system with rectangular voltage barriers has advantages both for technical applications and for analytical calculations of particle phase dynamics (simplifying significantly the last ones). Due to this reasons we consider mainly this options. Nevertheless, a few examples with barriers of quasi-sinusoidal form are given.

1. STACK PHASE ZONE, SEPARATRIX PARAMETERS AT RECTANGULAR BARRIERS

Let's consider particle motion inside the phase interval $\{0, \varphi_s\}$ (Fig. 1) in the absence of acceleration (i.e. at constant magnetic field $B(t) = B = \text{const.}$) As we show below, the particle phase trajectory, at certain conditions, is represented by a closed loop, and particles can be stacked there. Inside a barrier the particle momentum shifts per one turn by the value

$$\Delta p_{\text{turn}}(\varphi) = \frac{ZeV(\varphi)}{\beta \cdot c}, \quad V(\varphi) = V \cdot f(\varphi), \quad f(\varphi) = \begin{cases} 1, \ 0 \le \varphi \le \Delta\varphi_B, \\ 0, \ \Delta\varphi_B < \varphi \le \Delta\varphi_B + \Delta\varphi_{BB}, \\ -1, \ \Delta\varphi_B + \Delta\varphi_{BB} < \varphi \le \varphi_s. \end{cases} \quad (1.1)$$

$$\varphi_s = 2\Delta\varphi_B + \Delta\varphi_{BB}.$$

Here βc is velocity of the equilibrium particle traveling in the ring, Ze is its charge, $\eta_\omega = 1/\gamma^2 - 1/\gamma_{tr}^2$ is so called slippage factor. For n turns in negative barrier momentum shift gets equal to

$$\Delta p_n = \Delta p - n \cdot \delta p_B, \quad \delta p_B = \frac{ZeV}{\beta \cdot c}. \qquad (1.2)$$

Below when we consider barrier voltage of quasi-sinusoidal form this Formula for δp_B is used as well, but the symbol V designates the voltage amplitude. Here Δp is particle momentum shift (PMS further) when the particle moves between the barriers. As we see from (1.2), at

$$n = N \equiv \frac{\Delta p}{\delta p_B} \gg 1 \qquad (1.3)$$

PMS Δp_n changes its sign and the particle changes direction to the left-directed of its motion in phase space (Fig. 1). Entering the positive (left) barrier particle accelerates and, correspondingly, its momentum increases algebraically. As result, after the next N turns PMS becomes positive and phase drift direction changes to right-directed. For N turns particle phase shift (inside any of two barriers) is equal to

$$\Delta \varphi_N = \sum_{n=1}^{N} \Delta \varphi_n, \quad \Delta \varphi_n = \eta_\omega \omega_s \frac{\Delta p_n}{p_s} \cdot T_s = 2\pi \eta_\omega \cdot \frac{\Delta p_n}{p_s}, \quad \eta_\omega = \frac{1}{\gamma^2} - \frac{1}{\gamma_{tr}^2}. \qquad (1.4)$$

Here index s designates equilibrium particle and its orbit parameters, η_ω is so called *slippage factor* of the ring focusing system, γ is Lorenz-factor of equilibrium particle, p_s is its momentum, γ_{tr} is Lorenz-factor value corresponding to particle transition energy for the ring lattice, $\omega_s/2\pi$ and T_s are frequency and period of equilibrium particle revolution in the ring, correspondingly.

We consider here, for definition, the case of particle energy below transition value, i. e.

$$\gamma < \gamma_{tr}, \, \eta_\omega > 0.$$

Substituting in (1.4) the expression for Δp_n (1.2) and calculating the sum over n we find the particle phase shift for N turns:

$$\Delta \varphi_N = \frac{2\pi \eta_\omega}{p_s} \cdot \left(N \cdot \Delta p - \frac{N(N+1)}{2} \cdot \delta p_B \right).$$

3
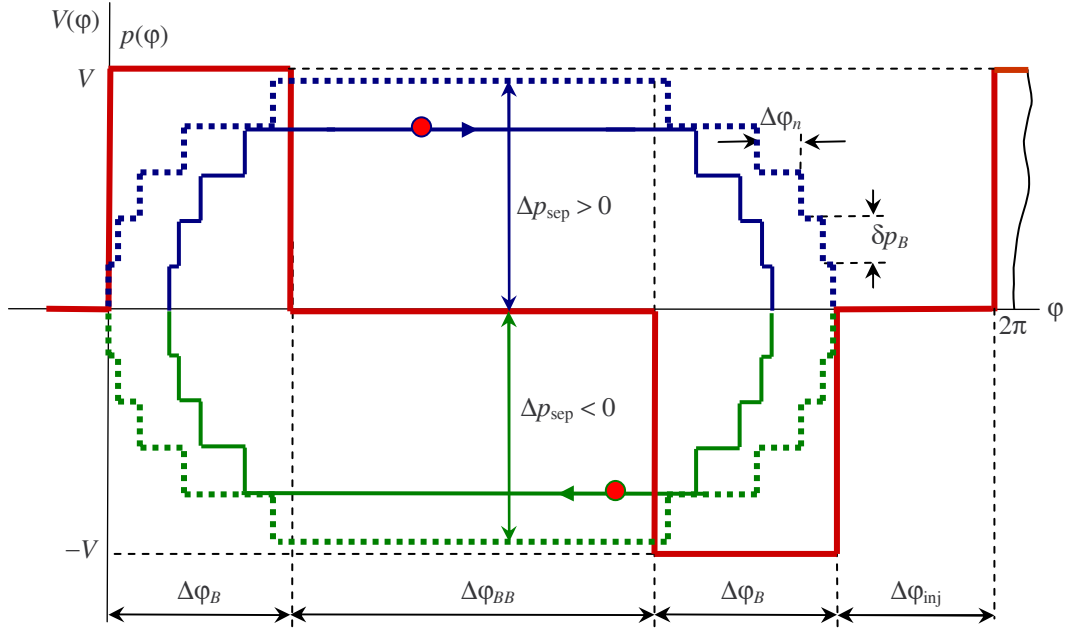
Fig. 1. Scheme of particle motion in the stable phase area $\Delta\varphi_{BB}$ and in positive and negative barriers; bold solid curve — barrier potential $V(\varphi)$; solid curve — phase trajectory of an stable particle $p(\varphi)$, the dot line — the same on separatrix; $p(\varphi)$ and $V(\varphi)$ in arb. units; arrows indicate momentum shift direction ($\eta_\omega > 0$)

For further description it is convenient to introduce the parameter equal to particle phase shift corresponding to δp_B:

$$\delta\varphi_B = 2\pi\eta_\omega \cdot \frac{\delta p_B}{p_s} = 2\pi\eta_\omega \cdot \frac{ZeV}{\beta^2\gamma Am_n c^2}. \tag{1.5}$$

Here A is particle atomic weight, m_n is nucleon mass. Then substituting $\Delta p = N \cdot \delta p_B$ into formula for $\Delta\varphi_N$ above we have

$$\Delta\varphi_N = N(N+1) \cdot \frac{\delta\varphi_B}{2}. \tag{1.6}$$

Particle does not cross the barrier if

$$\Delta\varphi_N \leq \Delta\varphi_B.$$

That is *necessary condition of separatrix existence*. Substituting here $\Delta\varphi_N$ from (1.6) we find the exact number of turns for a particle on separatrix:

$$N = \frac{1}{2} \cdot \left(\sqrt{1 + 8\frac{\Delta\varphi_B}{\delta\varphi_B}} - 1 \right) \approx \sqrt{2 \cdot \frac{\Delta\varphi_B}{\delta\varphi_B}}, \quad \Delta\varphi_B \gg \delta\varphi_B. \tag{1.7}$$

4

(see comments to Formula (1.12) below). Then the PMS on separatrix between the barriers (see Fig. 1 and equation (1.3)) is equal to

$$|\Delta p|_{\text{sep}} = N \cdot \delta p_B. \tag{1.8}$$

For δp_B (1.1) one can write from (1.8) the value of *PMS on separatrix* (between the barriers!):

$$\left| \frac{\Delta p}{p_s} \right|_{sep} = \frac{1}{\pi\eta_\omega} \sqrt{\frac{\Delta\varphi_B \cdot \delta\varphi_B}{2}} = \frac{1}{\beta} \cdot \sqrt{\frac{Z}{A} \cdot \frac{eV}{\eta_\omega \gamma m_n c^2} \cdot \frac{\Delta\varphi_B}{\pi}}. \tag{1.9}$$

It is noteworthy that the last expression in (1.9) by $\sqrt{2}$ less that classic one for $\left|\Delta p / p_s\right|_{\text{sep}}$ in the case of harmonic RF voltage.

Rewriting this equation for the barrier height V we find

$$V \geq \frac{A}{Z} \cdot \eta_\omega \beta^2 \gamma \cdot \frac{m_n c^2}{e} \cdot \frac{\pi}{\Delta\varphi_B} \cdot \left(\frac{\Delta p}{p} \right)^2_{sep}. \tag{1.10}$$

Particle synchrotron oscillation on separatrix

In the phase interval $\Delta\varphi_{BB}$ particle phase shift per turn (on separatrix) is, obviously, constant and equal to (compare (1.4))

$$\delta\varphi_{BB} = 2\pi\eta_\omega \left| \frac{\Delta p}{p} \right|_{sep}. \tag{1.11}$$

Then, its period of full turn on separatrix is

$$T_{\text{sep}} = 2T_s \cdot \left(\frac{\Delta\varphi_{BB}}{\delta\varphi_{BB}} + 2N \right) = T_s \sqrt{\frac{2}{\Delta\varphi_B \cdot \delta\varphi_B}} \cdot \left(4 \cdot \Delta\varphi_B + \Delta\varphi_{BB}\right). \tag{1.12}$$

Thus, the period on the separatrix in BB system with rectangular barriers has a finite value, as opposed to the case of harmonic RF voltage [5]. That is result of application of idealized rectangular barrier voltage form with rising and falling edges of infinite steepness. For real barrier voltage pulses the period on separatrix is infinitely long. We consider this problem in detail in the section 2.2 (see (2.22)). Nevertheless, the result obtained for rectangular barriers is valuable for simple estimates (see Fig. 2).

It is useful to write one more expression for $\delta\varphi_B$ to be used hereafter:

$$\delta\varphi_B = \pi^2 \eta_\omega^2 \frac{2}{\Delta\varphi_B} \cdot \left(\frac{\Delta p}{p} \right)^2_{sep}. \tag{1.13}$$
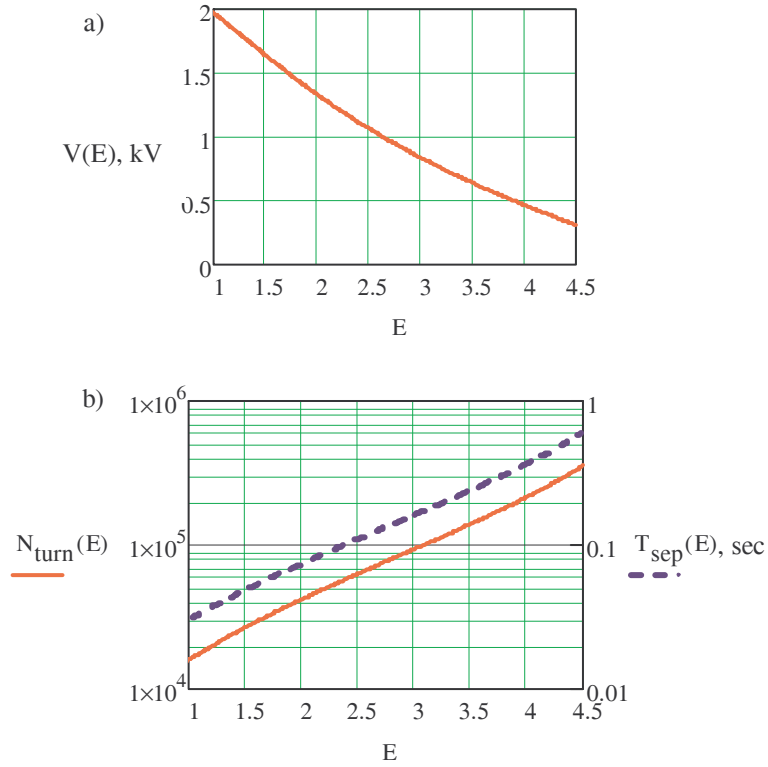
Fig. 2. Separatrix parameters: a) Barrier voltage $V(E)$ (1.10) vs ion energy (GeV/u); b) turn number (solid curve) and period (sec, dashed curve) of particle oscillation on separatrix vs ion energy (GeV/u); the following parameter values are used: particles — $^{197}\text{Au}^{79+}$, $C_{Ring} = 503$ м, $\gamma_{tr} = 7.09$, $|\Delta p/p_s| = 5 \cdot 10^{-4}$, rectangular barriers: $\Delta\varphi_B = \pi/10$, $\Delta\varphi_{BB} = 1.3 \cdot \pi$ [*]

2. GENERAL CASE OF THE BARRIERS OF ARBITARY FORM

2.1. Equations of particle traveling in phase space

From previous consideration one can derive differential equations for the case of barrier voltage of general form similar to those ones of particle motion at harmonic RF voltage action (see equations (1.1), (1.4)):

$$V(\varphi) = V \cdot f(\varphi), \quad |f(\varphi)| \leq 1, \tag{2.1}$$

$$\frac{dp(t)}{dt} = \frac{ZeV}{C_{Ring}} \cdot f(\varphi), \tag{2.2}$$

_____

[*] These parameter values will be used in all numerical examples below.

6

$$\frac{d\varphi(t)}{dt} = \omega - \omega_s = \omega_s \eta_\omega \frac{p(t) - p_s(t)}{p_s}. \qquad (2.3)$$

Here $V = V_{\max}(\varphi)$, $f(\varphi)$ is function describing phase dependence of $V(\varphi)$ function, $C_{Ring} = \beta c T_s$ is the ring circumference. These equations are valid both at constant magnetic field of the accelerator and when magnetic field changes in time. We'll consider the last case in section 4.

Introducing dimensionless parameters

$$\psi = \sqrt{\delta\varphi_B} \cdot \frac{t}{T_s}, \quad Y(\psi) = \frac{2\pi\eta_\omega}{\sqrt{\delta\varphi_B}} \cdot \frac{\Delta p(\psi)}{p_s}, \qquad (2.4)$$

where $\delta\varphi_B$ is defined with Formulae (1.5), (1.13) we obtain from (2.2), (2.3) the following equations:

$$\frac{dY}{d\psi} = f(\varphi), \qquad (2.5)$$

$$\frac{d\varphi}{d\psi} = Y, \qquad (2.6)$$

$$\frac{d^2\varphi}{d\psi^2} = f(\varphi). \qquad (2.7)$$

The variables $Y(\psi)$ and $\varphi(\psi)$ are canonically conjugated with Hamiltonian

$$\mathcal{H} = \frac{Y^2}{2} - \int f(\varphi) \cdot d\varphi . \qquad (2.8)$$

In other words,

$$W(\psi) = Y^2/2 \quad \text{and} \quad U(\varphi) = -\int f(\varphi) \cdot d\varphi \qquad (2.9)$$

are particle kinetic and potential energy. Correspondingly, $Y(\psi)$ and $\varphi(\psi)$ are particle momentum and co-ordinate and ψ is analogue of time. From the equation (2.5)÷(2.7) follows that the functions $Y(\psi)$ and $\varphi(\psi)$ depend only on form of function $f(\varphi)$, i. e. on form of barrier voltage. In such a sense, these functions are *universal solution* of those equations. The expression (2.8) allows us to derive general solution of the equations (2.5)÷(2.7) in variables $Y(\varphi)$, φ:

$$Y(\varphi) = \pm\sqrt{Y_0^2 + 2\int_{\varphi_0}^{\varphi} f(\phi) \cdot d\phi}, \quad 0 \le \varphi \le 2\pi. \qquad (2.10)$$

Here $Y_0 = Y(\varphi_0)$. The sign "+" is to be chosen at $Y(\varphi_0) > 0$, and backwards.

Formula for Hamiltonian can be obtained easily if to write equation (2.5) in the form

$$\frac{dY}{d\varphi} \cdot \frac{d\varphi}{d\psi} = f(\varphi),$$

and substitute here $d\varphi/d\psi$ from (2.6). Then, after integration we come to (2.8), where $\mathcal{H}$ is constant of integration.

One should note that defined in (1.5) parameter $\delta\varphi_B$ can be rewritten as $\delta\varphi_B = \left(\Omega_{synch} \cdot T_s\right)^2$, where Ω_{synch} is frequency of linear synchrotron oscillations of particles in the field of harmonic RF system at harmonics number $h = 1$. Therefore one can say that ψ is the phase of particle synchrotron oscillation in BB RF system and (2.7) is an analogue of well-known *equation of synchrotron oscillation* in harmonic RF system (see Ref. 5, Chapter IV).

Form of potential function $U(\varphi)$ in Fig. 3 clearly shows existing of potential well where particles can be stacked. The condition of particle catching in the stacking phase area, or the condition of particle motion phase stability is, evidently, as following:

$$\mathcal{H} \leq 0.$$
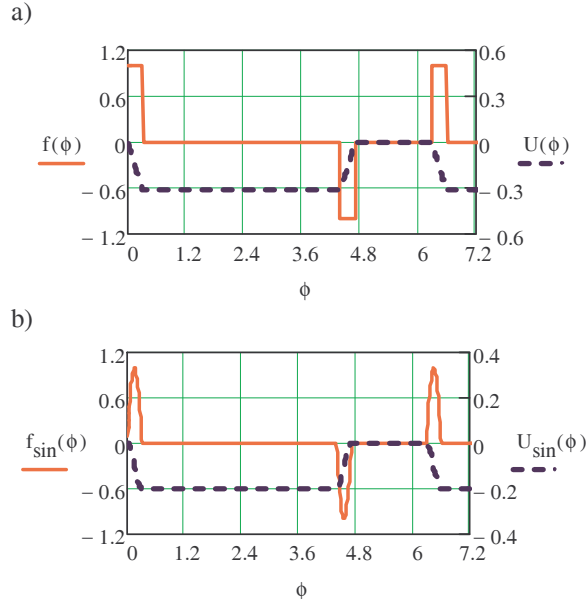
Fig. 3. Functions $f(\varphi)$ (solid lines) and $U(\varphi)$ (dashed lines) for rectangular barriers (a) and quasi-sinusoidal ones (b); $\Delta\varphi_B = \pi/10$, $\Delta\varphi_{BB} = 1.3\pi$

Phase trajectory of a stacked particle has form of a closed loop. The turning point φ_{max} can be found from the equation (2.10) if we choose there $Y_0 = 0$. Then we come to the equation

$$\int_{\varphi_0}^{\varphi_{\max}} f(\varphi) \cdot d\varphi = 0. \tag{2.11}$$

For the rectangular barriers of equal height V (Fig. 1, 3, a) it gives us

$$\varphi_{\max} = 2 \cdot \Delta\varphi_B + \Delta\varphi_{BB} - \varphi_0. \tag{2.12}$$

The separatrix phase span corresponds to $\varphi_0 = 0$, $\varphi_{\max} = \varphi_s$ that agrees with results of Section 1.

At $\mathcal{H} > 0$ particle injected in $\Delta\varphi_{\text{inj}}$ phase area $\left(U(\varphi_{\text{inj}}) = 0\right)$ with any nonzero momentum $\left|Y_{\text{inj}}\right| > 0$ passes stack area and continues travelling along abscissa in phase area indefinitely long. To catch it into stack potential well one needs to decrease its total energy to the level of $\mathcal{H} < 0$, i. e. one needs to have some "*cooling*" mechanism. We consider this procedure in the Section 3.

The equation (2.7) has a well known general solution for the case of arbitrary function $f(\varphi)$:

$$\psi(\varphi) = \int_{\varphi_0}^{\varphi} \frac{d\chi}{\sqrt{2 \int_{\varphi_0}^{\chi} f(\xi) \cdot d\xi + \left(\varphi'(\varphi_0)\right)^2}}, \quad \psi(\varphi_0) = 0. \tag{2.13}$$

Here, as before, φ_0 is initial phase value. For the case of a piecewise smooth function $f(\varphi)$ like in the case of the RF barrier voltage one has to solve the equation (2.7) sequentially, piece by piece, and matching solution at the borders of the pieces. The simplest way to do it is finding the first integral of the equation (2.7) that is equal to denominator of the expression under integral in (2.13). Simultaneously it is equation of phase trajectory (2.10) in (Y, φ) variables (i. e. for both $\mathcal{H} \le 0$ and $\mathcal{H} > 0$ in (2.8)). Particularly, if we have chosen $Y_0 = 0$ the solution (2.10) for the *rectangular barriers* at the stack area ($\mathcal{H} \le 0$) gives us

$$Y(\varphi) = \pm \begin{cases} \sqrt{2(\varphi - \varphi_0)}, & \varphi_0 \le \varphi \le \Delta\varphi_B, \\ \sqrt{2(\Delta\varphi_B - \varphi_0)}, & \Delta\varphi_B \le \varphi \le \Delta\varphi_B + \Delta\varphi_{BB}, \\ \sqrt{2(\varphi_s - \varphi_0 - \varphi)}, & \Delta\varphi_B + \Delta\varphi_{BB} \le \varphi \le \varphi_s - \varphi_0. \end{cases} \tag{2.14}$$

9

The barrier voltage function for quasi-sinusoidal barriers (Fig. 3, b) is

$$
f(\varphi) = \pm
\begin{cases}
\sin\left(\pi \cdot \dfrac{\varphi}{\Delta\varphi_B}\right), & 0 \le \varphi \le \Delta\varphi_B; & (I) \\[2mm]
0, & \Delta\varphi_B \le \varphi \le \Delta\varphi_B + \Delta\varphi_{BB}; & (II) \\[2mm]
-\sin\left(\pi \cdot \dfrac{\varphi - (\Delta\varphi_B + \Delta\varphi_{BB})}{\Delta\varphi_B}\right), & \Delta\varphi_B + \Delta\varphi_{BB} \le \varphi \le \varphi_s. & (III)
\end{cases}
$$

Integrating (2.10) with this function at $Y_0 = 0$ we find

$$
Y(\varphi) = \pm\sqrt{\frac{2 \cdot \Delta\varphi_B}{\pi}}
\begin{cases}
\sqrt{\cos\dfrac{\pi\varphi_0}{\Delta\varphi_B} - \cos\dfrac{\pi\varphi}{\Delta\varphi_B}}\,, & \varphi_o \le \varphi \le \Delta\varphi_B, \\[3mm]
\sqrt{\cos\dfrac{\pi\varphi_0}{\Delta\varphi_B} + 1}\,, & \Delta\varphi_B \le \varphi \le \Delta\varphi_B + \Delta\varphi_{BB}, \\[3mm]
\sqrt{\cos\dfrac{\pi\varphi_0}{\Delta\varphi_B} - \cos\dfrac{\pi(\varphi - \Delta\varphi_B - \Delta\varphi_{BB})}{\Delta\varphi_B}}\,, \\[3mm]
\quad \Delta\varphi_B + \Delta\varphi_{BB} \le \varphi \le \varphi_s - \varphi_0.
\end{cases}
\tag{2.15}
$$

For separatrix we have $\varphi_0 = 0$, $Y_0 = 0$, $f(0) = 0$ (dot curve in Fig. 1), and from (2.14), (2.15) we obtain the values of Y_{sep} between the barriers:

$$
Y_{\text{sep}} = \pm
\begin{cases}
\sqrt{2 \cdot \Delta\varphi_B}\,, & \text{rectangular\ barriers}, \\[3mm]
2 \cdot \sqrt{\dfrac{\Delta\varphi_B}{\pi}}\,, & \text{quasi-sinusoidal\ barriers},
\end{cases}
\quad \Delta\varphi_B \le \varphi \le \Delta\varphi_B + \Delta\varphi_{BB}. \tag{2.16}
$$

The first expression here leads, after substitution of $Y(\psi)$ from (2.4), to the Formula (1.9). For *quasi-sinusoidal barriers* we obtain similarly

$$
\left|\frac{\Delta p(\varphi)}{p_s}\right|^{\sin}_{\text{sep}} = \frac{\sqrt{\delta\varphi_B \cdot \Delta\varphi_B}}{\pi^{3/2}\eta_\omega} = \frac{1}{\beta\pi} \cdot \sqrt{\frac{Z}{A} \cdot \frac{2eV}{\eta_\omega\gamma m_n c^2} \cdot \Delta\varphi_B}\,,
$$

$$
V_{\sin} \ge \frac{A}{Z} \cdot \eta_\omega\beta^2\gamma \cdot \frac{m_n c^2}{e} \cdot \frac{\pi^2}{2\Delta\varphi_B} \cdot \left(\frac{\Delta p}{p}\right)^2_{\text{sep}}.
\tag{2.17}
$$

As follows from (2.16), (2.17) the value for PMS on separatrix at quasi-sinusoidal barriers less than that one at the rectangular barriers by the factor of $\sqrt{\pi/2}$ and the value of $V_{\sin}$ exceeds V (1.10) by the factor $\pi/2$ (that corresponds to ratio of integrals of $f(\varphi)$ over $\Delta\varphi_B$ phase interval for rectangular and quasi-sinusoidal barriers).

10

The expressions (2.14), (2.15) allow us to calculate the emittance of bunch stacked between two barriers:

$$\varepsilon_{stack}(\varphi_0) = 2 \int_{\varphi_0}^{2\pi-\varphi_0} Y(\phi) \cdot d\phi, \quad Y(\varphi) > 0. \tag{2.18}$$

Factor 2 appears here owing to symmetry of the outer phase trajectory relatively to the abscissa in Fig. 1. For *rectangular barriers* a simple integration gives us

$$\varepsilon_{stack}(\varphi_0) = 2\sqrt{2}\left[\frac{4}{3}(\Delta\varphi_B - \varphi_0)^{3/2} + \sqrt{\Delta\varphi_B - \varphi_0} \cdot \Delta\varphi_{BB}\right],$$

$$\varepsilon_{stack}(Y_{max}) = 2 \cdot \left(\frac{4}{3}Y_{max}^3 + Y_{max}\Delta\varphi_{BB}\right), \quad Y_{max} \equiv \sqrt{2 \cdot (\Delta\varphi_B - \varphi_0)}. \tag{2.19}$$

Here Y_{max} is $Y(\varphi)$ value between the barriers on the outer phase trajectory.

Knowing solution $Y(\varphi)$ one can find *second integral* of the equation (2.7) and a time-dependent (ψ-dependent) solution in variables $Y(\psi)$, $\varphi(\psi)$. It make possible calculation of particle period travelling along phase trajectory. We postpone consideration of this problem to the Sections 2.2 and 3.

2.2. Particle trajectory inside separatrix

Analytical solutions exist, as usually, for a few particular cases, like rectangular and quasi-sinusoidal barriers (as we saw above), for harmonic RF, etc. Most efficient way to analyze particle dynamics in BB RF system is numerical solution of the equations (2.5)÷(2.7) in dimensionless variables Y, φ, ψ. Then, using universal functions $Y(\psi)$ and $\varphi(\psi)$ for given barrier function $f(\varphi)$ one can calculate concrete characteristics.

As an example we consider in this Section the case of rectangular barriers (1.1) with parameters of the function $f(\varphi)$ described in the caption of Fig. 4. We mentioned already that synchrotron tune on separatrix should be infinitely long. Indeed, if we inject particle in the point $\varphi_{inj} = 0$ with PMS $\Delta p_{inj} = 0$ it will not move at all (because $V(0) = 0$). Then a small nonzero PMS or $\varphi_{inj} \neq 0$ provides a particle motion along *phase trajectory close to separatrix* (PTCS). An exception exists for rectangular barriers if $f(\varphi) = 1$ at $\varphi = 0$. It is, as mentioned above, an "idealized case" of barrier voltage pulses with indefinitely steep edges (do compare Fig. 4 and Fig. 1).

11
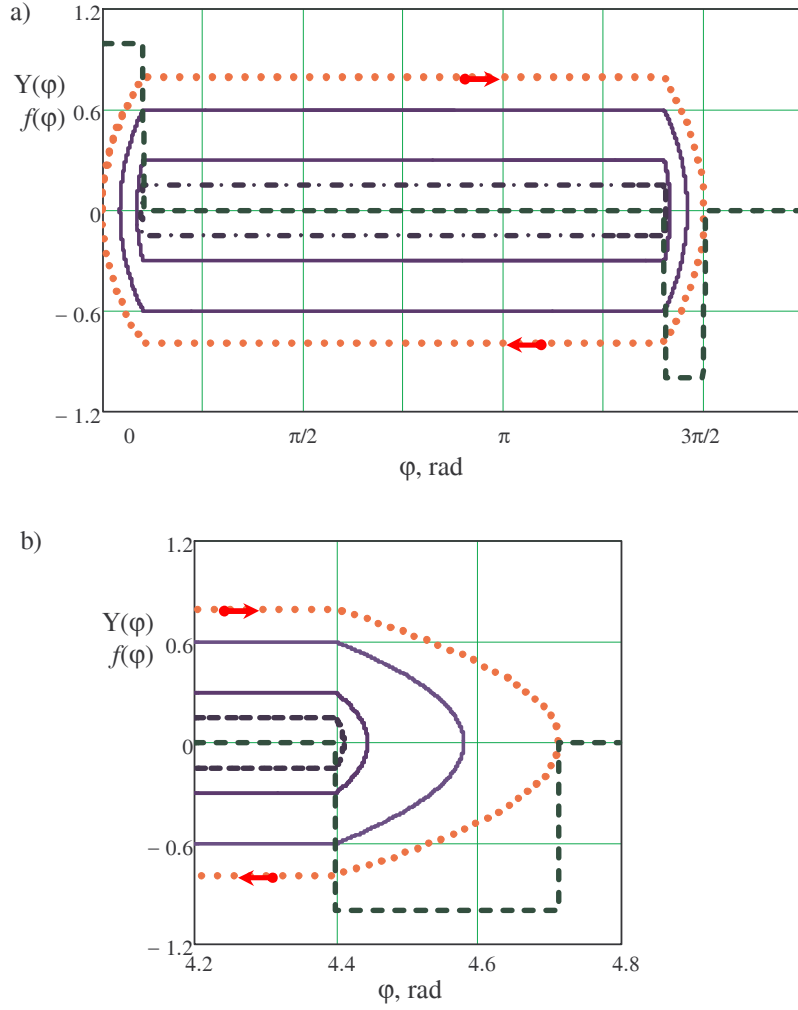
Fig. 4. Particle phase trajectories inside separatrix in the stable phase area (a) between positive and negative rectangular barriers and (b) inside negative barrier; dashed curve — the barrier voltage function $f(\varphi)$; dot line is normalized PMS (2.4) on separatrix calculated with equations (2.5), (2.6) in Mathcad at initial conditions $\varphi_0 = 0$, $Y_0 = 0$; two solid lines and dot-dashed one — the trajectories calculated at initial conditions (φ_0, Y_0) equal to $(\pi/2, 0.6)$, $(\pi, 0.3)$, $(4.2, 0.15)$ correspondingly; arrows indicate momentum shift direction $(\eta_\omega > 0)$; rectangular barrier buckets (see (1.10), $\Delta\varphi_B = \pi/10$, $\Delta\varphi_{BB} = 1.3\pi$

It clearly demonstrates, a propos, calculation with Mathcad Runge–Kulta solver: process stops if put $f(\varphi) = 1$ at $\varphi > 0$ and nicely operates if $f(\varphi) = 1$ at $\varphi \geq 0$.

For calculation of time of particle travelling along phase trajectory (synchrotron tune) one can use the equation (2.6) at given $Y(\varphi)$ (first integral of the equation (2.7)):

$$\Delta\psi_{period} = 2 \cdot \int_{\varphi_0}^{\varphi_s - \varphi_0} \frac{d\phi}{Y(\phi)}, \quad Y(\varphi) > 0. \tag{2.20}$$

12

Here we use again symmetry of phase trajectory (factor 2), φ_0 is initial phase where $Y(\varphi_0) = 0$. For rectangular barriers (2.14) we find by integration

$$\Delta\psi_{period} = \sqrt{\frac{2}{\Delta\varphi_B - \varphi_0}} \cdot (4 \cdot \Delta\varphi_B + \Delta\varphi_{BB} - 4 \cdot \varphi_0) = 4Y_{max} + \frac{2 \cdot \Delta\varphi_B}{Y_{max}},$$

$$T_{period} = T_s \sqrt{\frac{2}{\Delta\varphi_B \cdot \delta\varphi_B}} \cdot \left(\Delta\varphi_{BB} + 4 \cdot \Delta\varphi_B - \varphi_0\right).$$

$$(2.21)$$

For particle on separatrix $\varphi_0 = 0$ and we come again to (1.12). Thus, we have shown finally that "step by step" approach agrees with general one.

The case of quasi-sinusoidal barriers is more complicated. Indeed, similar integration of (2.20) with $Y(\varphi)$ from (2.15) results in logarithmic dependence of $\Delta\psi_{period}$ on φ_0. This fact is confirmed with numerical integration of the equations (2.5), (2.6) for quasi-sinusoidal $f(\varphi)$, as Fig. 5 shows. One can see the logarithmic growth of the travelling period (in ψ units) with φ_0 decrease, similar to the case of harmonic RF voltage [5]:

$$\Delta\psi_{period} \approx 13.7 - \ln\varphi_0. \qquad (2.22)$$

The difference we see between rectangular barriers (1.12), (2.21) and quasi-sinusoidal ones is related to mentioned above steepness of the barrier pulse edges. For quasi-sinusoidal barriers a particle at $\varphi^* = \{0, \varphi_s\}$ does not move at all if its momentum at this points is equal to zero (on separatrix!) because $f(\varphi^*) = 0$ exactly. For "idealized" rectangular barriers discussed above we have uncertainty that does not influence at analytical integration or "step by step" approach due to finite step value.
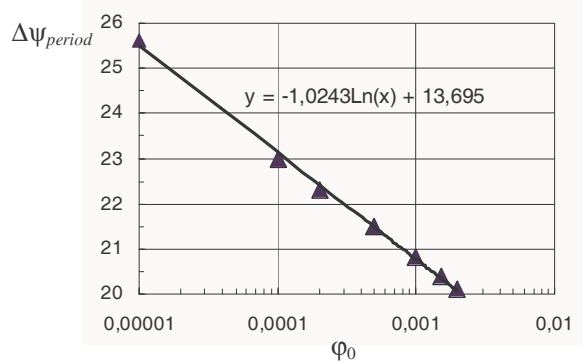
Fig. 5. Dependence of $\Delta\psi_{period}$ (particle synchrotron tune) on initial point coordinate φ_0 near the point $\varphi = 0$ calculated with equations (2.5), (2.6) in Mathcad for quasi-sinusoidal function $f(\varphi)$ at $\Delta\varphi_B = \pi/10$, $\Delta\varphi_{BB} = 1.3\pi$; the trend formula is shown in the diagram

13

Knowing the value of Y(φ) for given function $f(\varphi)$ one can find concrete parameter values for this case. For instance, *the amplitude of barrier voltage* is expressed according to Formula (2.4) via Y_{max} and other parameters as following:

$$V \geq \frac{A}{Z} \cdot \eta_\omega \beta^2 \gamma \cdot \frac{m_n c^2}{e} \cdot \frac{2\pi}{Y_{max}^2} \cdot \left(\frac{\Delta p}{p} \right)^2_{sep}. \qquad (2.23)$$

Here Y_{max} is the Y value on PTCS between the barriers, at arbitrary barriers form.

3. STACKING (RECTANGULAR BARRIERS)

Formation of intense particle beams in cyclic accelerators is performed often with application of repeated injection cycles at certain periodicity and storage injected particle bunches — so called *stacking*. We consider now the stacking process for the case of rectangular barriers using results of Section 2.

3.1. Particle phase travelling period at stacking

First we expand the phase area up to $\varphi = 2\pi$ (see Fig. 1, 6) and have

$$f(\varphi) = \begin{cases} 1, & 0 \leq \varphi \leq \Delta\varphi_B, & (I) \\ 0, & \Delta\varphi_B < \varphi \leq \Delta\varphi_B + \Delta\varphi_{BB}, & (II) \\ -1, & \Delta\varphi_B + \Delta\varphi_{BB} < \varphi < \varphi_s, & (III) \\ 0, & \varphi_s \equiv 2\pi - \Delta\varphi_{inj} < \varphi \leq 2\pi. & (IV) \end{cases} \qquad (3.1)$$

As we mentioned in the Section 2.1 a particle injected into $\Delta\varphi_{inj}$ phase area travels along φ-axis without limitation. In this case it undergoes some periodic oscillations of momentum (Y(φ)) when passing through the barriers (Fig. 6). One can calculate parameters of these oscillations using same method as in previous section. First we calculate Y(φ) with (2.10) over interval $\varphi_0 \leq \varphi \leq \varphi_0 + 2\pi$ at the condition that initial (injection) phase value φ_0 spans in the injection space area $\Delta\varphi_{inj}$ (Fig. 1, 6). Particle momentum inside this area is constant (and equal Y_0). Therefore a choice of φ_0 value does not change Y(φ) magnitude and integration in (2.10) one can perform along the span $0 \leq \varphi \leq 2\pi$. As result we find

14

$$Y(\varphi) = \frac{Y_0}{|Y_0|} \cdot \begin{cases} \sqrt{Y_0^2 + 2\varphi}, & 0 \leq \varphi \leq \Delta\varphi_B, & (I) \\ \sqrt{Y_0^2 + 2 \cdot \Delta\varphi_B}, & \Delta\varphi_B < \varphi \leq \Delta\varphi_B + \Delta\varphi_{BB}, & (II) \\ \sqrt{Y_0^2 + 2(\varphi_s - \varphi)}, & \Delta\varphi_B + \Delta\varphi_{BB} < \varphi \leq \varphi_s, & (III) \\ Y_0 & 2\pi - \Delta\varphi_{inj} < \varphi \leq 2\pi. & (IV) \end{cases} \tag{3.2}$$
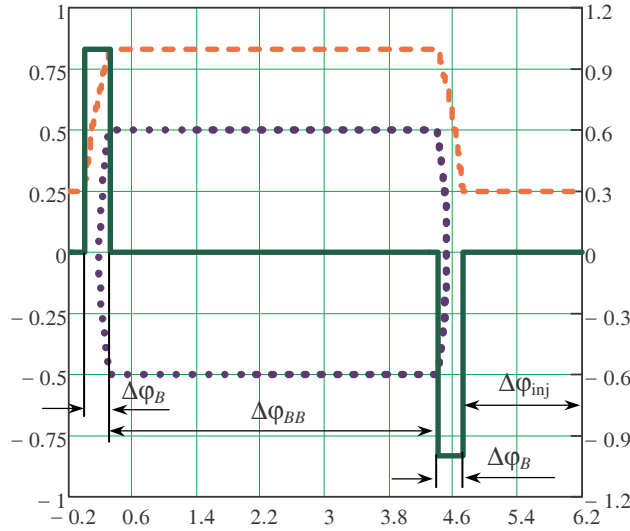
Fig. 6. Phase trajectories of injected particle (dashed line, $\varphi_{inj} = -0,2$, $Y_{inj} = 0,25$) and stacked one (dot line, $Y_{max} = 0,5$); $f(\varphi)$ is shown with solid curve

With this result found one can calculate period of injected particle oscillation using equation (2.6) similarly to (2.20), (2.21) and choosing initial point at the end of $\Delta\varphi_{inj}$ area (i. e. $\varphi_0 = 0$):

$$\Delta\psi_{period} = \int_0^{2\pi} \frac{d\phi}{Y(\phi)} = 2\sqrt{Y_0^2 + 2 \cdot \Delta\varphi_B} + \frac{\Delta\varphi_B}{\sqrt{Y_0^2 + 2 \cdot \Delta\varphi_B}} - 2Y_0 + \frac{\Delta\varphi_{inj}}{Y_0}. \tag{3.3}$$

3.2. Sufficient condition for particle stacking

Comparing the results (3.2) with (2.16) we see that for any value of particle injection momentum Y_0 its momentum in $\Delta\varphi_{BB}$ phase area (3.2, *II*) is larger that Y_{sep}. It means that phase trajectory of the particle injected into phase interval $\Delta\varphi_{inj}$ with momentum shift $\Delta p_{inj} \neq 0$ is not a closed loop (Fig. 6, dashed line). To be captured into *the stable phase* (*stack*) *area*

15

$$0 \le \varphi \le \varphi_s \tag{3.4}$$

one has to meet the condition

$$\left|Y_{BB}\right| \le \left|Y_{sep}\right|, \tag{3.5}$$

Were Y_{BB} is $Y(\varphi)$ value is the stack area. That is *the sufficient condition* for particle capture in the closed phase trajectory in stacking phase area.

This condition, as we have seen just above, is not met for particles injected into *unstable phase area* $\Delta\varphi_{inj}$. Thus, at any value of Y_0 the particle injected into unstable area $\Delta\varphi_{inj}$ can not be caught into stable area (3.4) and passes through it. To get caught the particle has to pass inside the positive or negative barrier at phase where its momentum shift $\Delta p_n = 0$ (see Fig. 1 and Fig. 6). Then it comes inside separatrix of stable phase trajectories. Only way to get such position (in the case of stationary barriers, see Section 5) is reduction of particle momentum after injection during particle travelling in phase space, i. e. a *cooling application*. Both *electron and stochastic cooling methods* are applicable for this purpose.

The last statement can be clearly explained with Fig. 3. Indeed, a particle injected into injection phase area $\Delta\varphi_{inj}$ has zero potential energy and total energy $\mathcal{H} > 0$. Due to this reason it can not be caught in potential well of the stable area $\Delta\varphi_{BB}$.

One can formulate the requirement to the cooling rate $(\tau_{cool})^{-1}$: during injection period T_{inj} reduction of PMS Δp_{BB} has to be sufficient for particle to enter inside separatrix of stable phase area $\Delta\varphi_{BB}$. One can assume exponential dependence of particle momentum on time (not always takes place):

$$\Delta p(t) = A \cdot \exp\{-t/\tau_{cool}\}, \quad A = \Delta p(0) = \Delta p_{BB},$$

where Δp_{BB} is PMS value inside the stable phase area at first passing $\Delta\varphi_{BB}$ area after injection. Then the *sufficient condition* of particle capture into stable phase area can be written as following:

$$\frac{\tau_{cool}}{T_{inj}} \le \left[\ln\left|\frac{\Delta p_{BB}}{\Delta p_{sep}}\right|\right]^{-1} = \left[\ln\left|\frac{Y_{BB}}{Y_{sep}}\right|\right]^{-1}. \tag{3.6}$$

16

Here Y_{BB} is described with Formula (3.2, *II*) and $Y_{sep} = \sqrt{2 \cdot \Delta\varphi_B}$ (see (2.16)). Substituting these formulae into (3.6) we find

$$\frac{\tau_{cool}}{T_{inj}} \leq 2 \cdot \left[\ln\left(1 + \frac{Y_0^2}{2 \cdot \Delta\varphi_B} \right) \right]^{-1} \sim \begin{cases} 2/\ln 2, & Y_0 \sim Y_{sep} \\ 4 \cdot \left(\dfrac{Y_{sep}}{Y_0} \right)^2, & Y_0 \ll Y_{sep}. \end{cases} \tag{3.7}$$

Thus, the most hard requirement of τ_{cool} value takes place at large Y_0 magnitude. And on the contrary, for small Y_0 magnitude the requirement is very soft. It is well understable: the smaller is Y_0 value of injected particle the nearer is its phase trajectory in $\Delta\varphi_{BB}$ phase area to the separatrix and the faster is catching of the particle inside separatrix.

3.3. Necessary condition for particle stacking

If PMS at injection Y_0 is sufficiently small the next limitation in the Y_0 value appears. Indeed, the PMS at injection has to be large enough to allow particle accomplishing at least one synchrotron oscillation during injection period T_{inj}:

$$T_{period} < T_{inj}. \tag{3.8}$$

If not the particle will be lost at the next injection pulse (when acceptance of the injection phase area is filled). Using the $\Delta\psi_{period}$ value (3.3) with Formula for ψ from (2.4) we come to nonlinear algebraic equation, which allows us to find minimal value of Y_0:

$$\Delta\psi_{period}(Y_0) = \frac{T_{inj}}{T_s} \cdot \sqrt{\delta\varphi_B}. \tag{3.9}$$

One can rewrite this formula to the form containing $(\Delta p / p)_{sep}$ that is characteristics of the stack area:

$$\Delta\psi_{period}(Y_0) = \pi\eta_\omega \frac{T_{inj}}{T_s} \sqrt{\frac{2}{\Delta\varphi_B}} \cdot \left| \frac{\Delta p}{p} \right|_{sep}. \tag{3.10}$$

17

A solution of the equation (3.10) for Y_0 can be found numerically. Then, knowing minimal allowed value of Y_0 we can calculate $(\Delta p/p)_{inj}$ — minimal PMS in injection area:

$$\left.\frac{\left|\Delta p_{inj}\right|}{p_s}\right|_{min} = \frac{(Y_0)_{min}}{\sqrt{2 \cdot \Delta\varphi_B}}.$$

(3.11)

An example of such calculation is presented in Fig. 7.
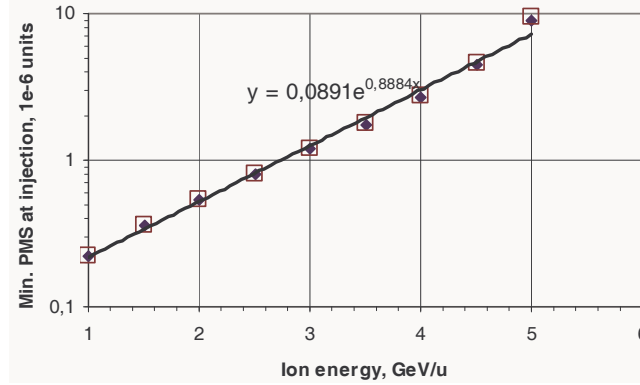
Fig. 7. Dependence of minimum $\left|\Delta p_{inj}\right|/p_s$ in 10^{-6} units on ion energy (Gev/u); the markers indicate calculation results for rectangular barriers with Formulae (3.10), (3.11) (diamonds) and approximate Formula (3.12) (empty squares); $\left.|\Delta p/p_s|\right|_{sep} = 5 \cdot 10^{-4}$; the parameters of the ring and the barrier scheme are the same as in previous examples, the injection period $T_{inj} = 10$ s; the Formula of the trend (solid curve) $y(E_{ion})$ is shown in the diagram

The calculation can be significantly simplified at $Y_0 \ll 1$ when $\Delta\psi_{period}(Y_0) \approx \Delta\varphi_{inj}/Y_0$. Substituting this value in (3.9) with Y from (2.4) we find the approximate formula

$$\frac{\left|\Delta p_{inj}\right|}{p_s} \geq \frac{\Delta\varphi_{inj}}{2\pi\eta_\omega} \cdot \frac{T_s}{T_{inj}} \cdot \left.\frac{\left|\Delta p\right|}{p_s}\right|_{sep}.$$

(3.12)

Parameter $\left.|\Delta p/p_s|\right|_{sep}$ here is actually characteristics of BB system via Formulae (1.9), (1.10). The results of calculations with (3.12) are in a good agreement with results of numerical solution described above. For parameters listed in caption to Fig. 7 at least both results coincide with accuracy of 1÷5 % depending of energy. One can conclude that the criterion (3.12) works well for simple estimates.

18

An example of experiment for studies of ion stacking with BB technique performed at GSI [10] is presented in Fig. 8.
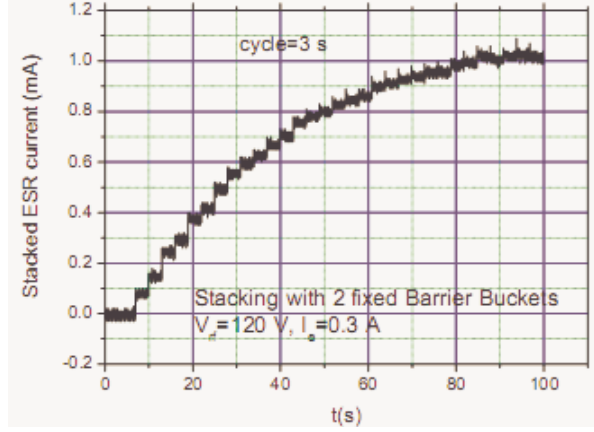
Fig. 8. Stacking of $^{124}Xe^{54+}$ ions in ESR [10] with two fixed barrier buckets at electron cooling. Saturation of stacked beam intensity can be explained by peculiarities of technical realization of the stacking scheme (see section 3.5)

3.4. Stacking with accelerating voltage at injection area

To avoid at stacking the loss of the particles having momentum below allowed minimum, as described in the previous section, it was proposed [16] to apply to injection phase area $\Delta\varphi_{inj}$ (Fig. 1, 6) a small voltage $V_{inj} \equiv k_{inj}V << V$. For instance, the function $f(\varphi)$ for rectangular barrier voltage in this case is described as follows:

$$f(\varphi) = \begin{cases} 1, & 2\pi n \le \varphi \le 2\pi n + \Delta\varphi_B, & (1) \\ 0, & 2\pi n + \Delta\varphi_B < \varphi \le 2\pi n + \Delta\varphi_B + \Delta\varphi_{BB}, & (2) \\ k, & 2\pi n + \Delta\varphi_B + \Delta\varphi_{BB} < \varphi \le 2\pi n + \varphi_s, & (3) \\ k_{inj}, & 2\pi n + \varphi_s < \varphi \le 2\pi(n+1). & (4) \end{cases} \quad (3.13)$$

Evidently, the function $f(\varphi)$ has to meet the following condition:

$$\int_0^{2\pi} f(\varphi) \cdot d\varphi = 0. \quad (3.14)$$

If not the unstacked (yet) particle accelerates passing the full phase span $0 \le \varphi \le 2\pi$ (see also Section 6). The condition (3.14) gives us the relation between parameters k and k_{inj}:

$$k = -\left(1 + \frac{\Delta\varphi_{inj}}{\Delta\varphi_B} \cdot k_{inj}\right). \quad (3.15)$$

19

The criterion of choice of k_{inj} value is described with the same Formula (3.8). It requires to calculate T_{period} as function of k_{inj}. This calculation is similar to the procedure of Formula (3.3) obtaining, but is rather cumbersome. However, a simple estimate of minimal value of k_{inj} can be done for *rectangular barriers* if we consider an outmost case of a particle injected at zero PMS into phase point φ_{inj} at the beginning of $\Delta\varphi_{inj}$ phase area (Fig. 9):

$$Y_0 = 0, \quad \varphi_{inj} = -\Delta\varphi_{inj}. \tag{3.16}$$

One has to underline that in Fig. 9 we shifted injection area into negative phase span. It was done to keep the stable phase area at the same phase span (3.4).
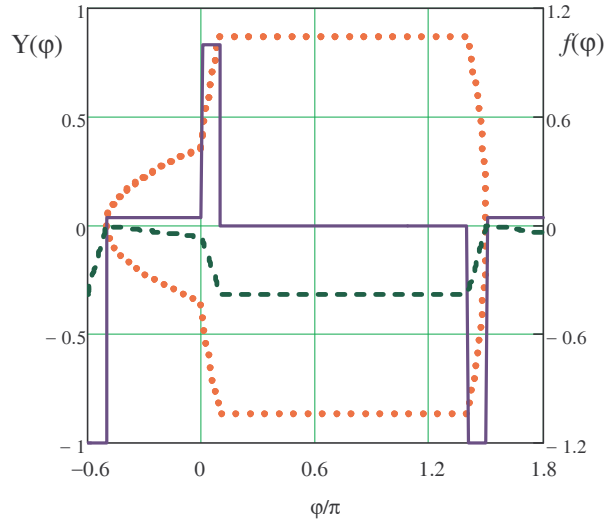
Fig. 9. Particle phase trajectory at stacking with rectagular barriers and additional acceleration voltage in phase area $\Delta\varphi_{inj}$; solid curve is the barrier function $f(\varphi)$ (3.13) at $k_{inj} = 0.04$, $k = -1.2$; dashed line is $U(\varphi)$ function (3.17); dot line is normalized PMS $Y(\varphi)$ (2.4) on phase trajectory calculated with equations (2.5), (2.6) in Mathcad; $\Delta\varphi_B = \pi/10$, $\Delta\varphi_{BB} = 1.3\cdot\pi$, particle injection parameters: $Y_0 = 0$, $\varphi_{inj} = -\Delta\varphi_{inj}$

The predominant contribution into particle oscillation period gives the time of its crossing of $\Delta\varphi_{inj}$ phase area. One can find easily (see Section 2) PMS in $\Delta\varphi_{inj}$ area and correspondingly ψ parameter span:

$$Y(\varphi^*) = \sqrt{2k_{inj}\cdot\varphi^*}, \quad \Delta\psi_{inj} \approx \sqrt{2\cdot\frac{\Delta\varphi_{inj}}{k_{inj}}}, \quad k_{inj} \ll 1, \quad 0 \le \varphi^* \le \Delta\varphi_{inj}. \tag{3.17}$$

Applying limitation (3.8) we find (using (3.10)) the minimal value of k_{inj}:

$$k_{inj} \ge \frac{\Delta\varphi_{inj}\Delta\varphi_B}{\pi^2\eta_\omega^2}\cdot\left(\frac{T_s}{T_{inj}}\right)^2\cdot\left(\frac{\Delta p}{p}\right)_{sep}^{-2}. \tag{3.18}$$

20

We see from numerical example (Fig. 10) the parameter k_{inj} grows up with energy when it approaches transition energy value.

The estimate (3.18) is an inferior limit. In reality one may require larger, by several times, k_{inj} magnitude. That occurs due to relatively fast drift of particle through $\Delta\varphi_{BB}$ area where it has big PMS. For correct value of k_{inj} parameter one has to perform numerical simulations.
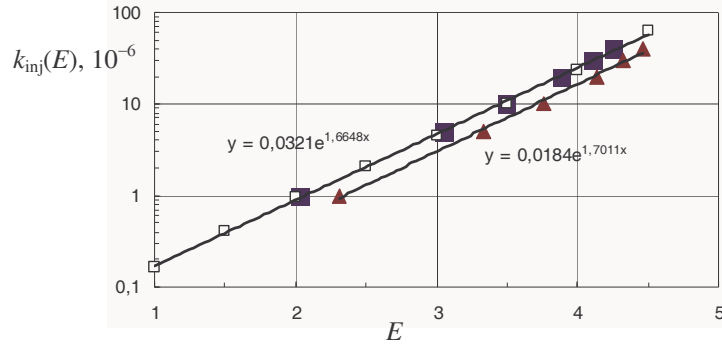
Fig. 10. Dependence of parameter k_{inj} (in 10^{-6} units) on energy (Gev/u). The ring and BB system parameters as in previous figures, $T_{inj} = 10$ s; large squares — rectangular barriers (3.13), numerical calculations of differential equations (2.5), (2.6), small empty squares — the same calculated with approximate Formula (3.18); triangles — sinusoidal barriers, numerical calculations of (2.5), (2.6); solid lines — trends, the Formulae are shown in the Figure

The peculiarity of the regime considered here shows the potential function (Fig.9)

$$
U(\varphi) = - \int_{-\Delta\varphi_{inj}}^{\varphi_s} f(\phi) \cdot d\phi =
$$

$$
= \begin{cases} - k_{inj}(\varphi + \Delta\varphi_{inj}), & -\Delta\varphi_{inj} \le \varphi \le 0, \\ -(k_{inj} \cdot \Delta\varphi_{inj} + \varphi), & 0 < \varphi \le \Delta\varphi_B, \\ -(k_{inj} \cdot \Delta\varphi_{inj} + \Delta\varphi_B), & \Delta\varphi_B < \varphi \le \Delta\varphi_B + \Delta\varphi_{BB}, \\ -[k_{inj} \cdot \Delta\varphi_{inj} + \Delta\varphi_B + k(\varphi - \Delta\varphi_B - \Delta\varphi_{BB})], & \Delta\varphi_B + \Delta\varphi_{BB} \le \varphi_s, \end{cases} \tag{3.19}
$$

$$
U(-\Delta\varphi_{inj}) = 0.
$$

This function forms potential well in all phase span (3.20)

$$
-\Delta\varphi_{inj} \le \varphi \le 2\pi - \Delta\varphi_{inj}. \tag{3.20}
$$

21

3.5. Barrier voltage ripples and parasitic separatrix

Imperfection of a system of barrier voltage generation can manifest itself in appearance of voltage ripples, which follow the main barrier peaks. Two typical examples of such imperfect barrier voltage functions and possible aftermath are demonstrated in Fig. 11. The ripples can form phase areas of "parasitic separatrixes" where injected particles can be trapped at certain condition, as it was observed in Ref. 10. Such trajectories have the form of closed loops (Fig. 11, a, b, curves 3, 4).

A rough estimate of the effect of particle trapping into parasitic separatrix can be made comparing square of phase space inside separatrix S_{sep} and parasitic one S_{ripple}. The first one is equal to (see (1.9))

$$S_{sep} = \left| \frac{\Delta p}{p_s} \right|_{sep} \cdot \left(\Delta\varphi_{BB} + 2 \cdot \Delta\varphi_B \right) \propto \sqrt{V \cdot \Delta\varphi_B} \cdot \left(\Delta\varphi_{BB} + 2 \cdot \Delta\varphi_B \right).$$

Similarly, the S_{ripple} size can be written as follows:

$$S_{ripple} = \left| \frac{\Delta p}{p_s} \right|_{sep}^{ripple} \cdot \Delta_{ripple} \propto \sqrt{V_{ripple} \cdot \Delta\varphi_{ripple}} \cdot \Delta_{ripple}.$$

Here V_{ripple} is the ripple voltage amplitude, $\Delta\varphi_{ripple}$ is the width of ripple voltage peak, Δ_{ripple} is length of ripple peaks in phase space. Assuming $\Delta\varphi_{ripple} \approx \Delta\varphi_B$ one can write a simple formula for the part ε of particles lost at injection and stacking:

$$\varepsilon \equiv \frac{S_{ripple}}{S_{sep}} \sim \sqrt{\frac{V_{ripple}}{V}} \cdot \frac{\Delta_{ripple}}{2 \cdot \Delta\varphi_B + \Delta\varphi_{BB}}. \tag{3.21}$$

That gives us the requirement to the barrier voltage quality

$$\frac{V_{ripple}}{V} < \left(\varepsilon \cdot \frac{2 \cdot \Delta\varphi_B + \Delta\varphi_{BB}}{\Delta_{ripple}} \right)^2 \sim \varepsilon^2. \tag{3.22}$$

For instance, barrier voltage system with parameters shown in Fig. 11, b ($2 \cdot \Delta\varphi_B + \Delta\varphi_{BB} = 4.71$ rad, $\Delta_{ripple} \approx 1$ rad) one has to provide $V_{ripple}/V < 2.2 \cdot 10^{-3}$ at 1 % particle loss.
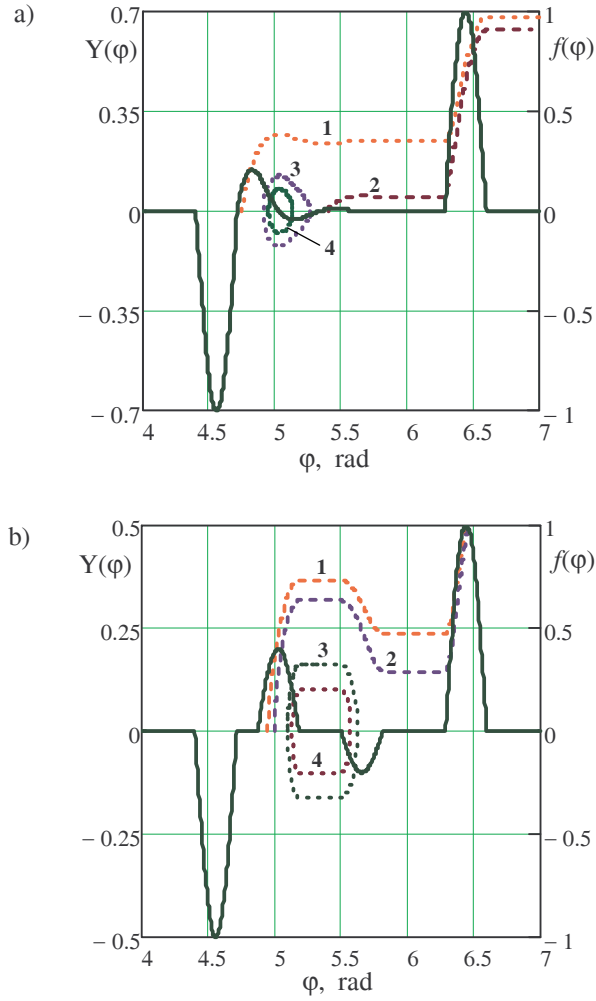
Fig. 11. Two examples of barrier voltage ripples and particle phase trajectories calculated with the equations (2.5), (2.6); main barrier peaks are quasi-sinusoidal followed with (a) exponentially fading oscillations (a) and (b) two sinusoidal peaks of decreasing amplitude; the injection parameters of n-th phase trajectory $(\varphi_{inj}, Y_{inj})_n$: a) $(4.75, 0.0)_1$, $(5.4, 0.0)_2$, $(5.0, 0.12)_3$, $(4.95, 0.0)_4$; b) $(4.95, 0.0)_1$, $(5.0, 0.0)_2$, $(5.1, 0.0)_3$, $(5.2, 0.1)_4$

4. PARTICLE ACCELERATION WITH BARRIER VOLTAGE

For particle acceleration with BB system one has to apply a voltage V_{acc} to the interval $\Delta\varphi_{BB}$ (Fig. 6). *Equilibrium particle* momentum should increase with time according to well-known equation

$$p_s(t) = \frac{ZeB_s(t)R_s}{c}. \tag{4.1}$$

23

Here $B_s(t)$ and R_s are magnetic field and trajectory radius averaged over the equilibrium trajectory. This equality allows us to derive the formula connecting the growing magnetic field $B_s(t)$ and accelerating voltage V_{acc}. Substituting

$$\frac{dp_s}{dt} = \frac{ZeR_s}{c} \cdot \frac{dB_s}{dt}$$

into the equality

$$\frac{dp_s}{dt} = \frac{\delta p_B}{T_s}$$

and δp_B from (1.2) we find desired formula:

$$V_{acc} = \frac{\rho C_{Ring}}{c} \cdot \frac{dB_\rho}{dt}. \tag{4.2}$$

Here $B_\rho = B_s R_s / \rho$ and ρ are magnetic field and equilibrium trajectory radius in dipoles, correspondingly. At the ring parameters $C_{Ring} = 503$ m, $\rho = 25$ m and magnetic field growth rate $dB_\rho / dt = 0.1\,\text{T/s}$ it requires $V_{acc} = 1.26$ kV.

The problem is not so trivial for *nonequilibrium particle*: $p(t) = p_s(t) + \Delta p$. If the condition (4.2) for V_{acc} is met the particle drifts between barriers, in $\Delta\varphi_{BB}$ phase area, having constant momentum shift $\Delta p(t) = \Delta p(0)$. It looks like the particle "does not feel" presence of accelerating voltage V_{acc}, because both nonequilibrium particle and equilibrium one get per turn the same energy ZeV_{acc} and, correspondingly, momentum δp_{acc} shifts. As result, a difference of their momenta remains constant. Therefore, in *first approximation*, the separatrix of particle phase trajectory is described, for instance, with the same Formulae (1.9), (2.13), (2.14) as at absence of acceleration. At the *second approximation* one has to take into account an influence of magnetic field growth when particle travels inside the barriers. This effect can be taken into account by introducing an *equivalent deceleration voltage* V_{dec} and corresponding it $f_{dec}(\varphi)$:

$$V_{dec} = -\frac{\rho C_{Ring}}{C} \cdot \frac{dB_\rho}{dt}, \quad f_{dec} = \frac{V_{dec}}{V} < 0, \quad 0 \le \varphi \le 2 \cdot \Delta\varphi_B + \Delta\varphi_{BB}. \tag{4.3}$$

Both functions are, generally speaking, depending of φ. Then the function $f(\varphi)$ used before can be presented as follows:

$$f(\varphi) = f_B(\varphi) + f_{dec}(\varphi), \tag{4.4}$$

where $f_B(\varphi)$ is the same, as before, the function of barrier voltage defined in (2.1) plus acceleration voltage (4.2).

Now the condition of particle motion phase stability (2.11) goes over

$$\int_0^{\varphi_s} f(\varphi) \cdot d\varphi = 0, \quad \text{or} \quad \int_0^{\varphi_s} f_B(\varphi) \cdot d\varphi = -\int_0^{\varphi_s} f_{\text{dec}}(\varphi) \cdot d\varphi. \qquad (4.5)$$

As an example we consider here the case of linear dependence of magnetic field B_ρ on time and rectangular barriers. Then both $V_{\text{acc}}(\varphi)$ and $f_{\text{dec}}(\varphi)$ are constant.

The simplest solution is to apply V_{acc} voltage (i. e. $\Delta f_B = -f_{\text{dec}} = \text{const}$) to all stable phase area (3.4). This addition provides particle acceleration compensating effect of growing B_ρ and trajectory of nonequilibrium particle has the same form as at absence of acceleration (Fig. 4). The peculiarity of such regime is position of *equilibrium phase*: it is the locus located on φ-axis, in the phase span $\Delta\varphi_B < \varphi < \Delta\varphi_B + \Delta\varphi_{BB}$.

Another solution (that can be suitable for some technical reasons) consists in an increase of acceleration voltage V_{acc} in $\Delta\varphi_{BB}$ phase area only by the addition

$$\Delta V_{\text{acc}} = \frac{2 \cdot \Delta\varphi_B}{\Delta\varphi_{BB}} \cdot V_{\text{acc}}, \quad \Delta f_B = \frac{\Delta V_{\text{acc}}}{V}, \quad \Delta\varphi_B < \varphi \le \Delta\varphi_B + \Delta\varphi_{BB}. \qquad (4.6)$$

It provides fulfillment of the conditions (4.5). Then the particle phase trajectory can be described as result of particle phase motion under the influence of

$$f(\varphi) = f_B(\varphi) + \Delta f_B(\varphi) + f_{\text{dec}}(\varphi).$$

In the case of rectangular barrier $f(\varphi)$ has the following view:

$$f(\varphi) = \begin{cases} 1 + f_{\text{dec}}, & 0 \le \varphi \le \Delta\varphi_B; \\ \Delta f_B, & \Delta\varphi_B < \varphi \le \Delta\varphi_B + \Delta\varphi_{BB}; \\ -1 + f_{\text{dec}}, & \Delta\varphi_B + \Delta\varphi_{BB} < \varphi \le \varphi_s; \\ 0, & \varphi_s < \varphi \le 2\pi. \end{cases} \qquad (4.7)$$

Fig. 12 demonstrates phase trajectories of accelerated particles at different injection parameters given in the Figure caption. One can see that the trajectories here have some similarity of forms with those ones at classic harmonic RF voltage acceleration [5]. The similarity is also in existence of single *equilibrium point* in this case: $Y_{equilibrium} = 0$, $\varphi_{equilibrium} = \Delta\varphi_B + \Delta\varphi_{BB}$. As we see from Fig. 12, the phase trajectory loop shrinks to this point as φ_{inj} approaches $\varphi_{equilibrium}$.

The phase trajectories have a form of closed loop and their parameters $Y(\psi)$, $\varphi(\psi)$ are insensitive directly to particle acceleration. It means that $Y(\psi)$ function for each trajectory is invariant of energy. Then, one can derive from (2.4) with (1.5) for any trajectory the value of PMS dependence on energy:

$$\frac{\Delta p(E,\psi)}{p_s} = \frac{Y(\psi)}{\beta(E)}\sqrt{\frac{ZeV}{2\pi\eta_\omega(E)\cdot\gamma(E)\cdot Am_nc^2}} \tag{4.8}$$

(do compare [5], p. 159).
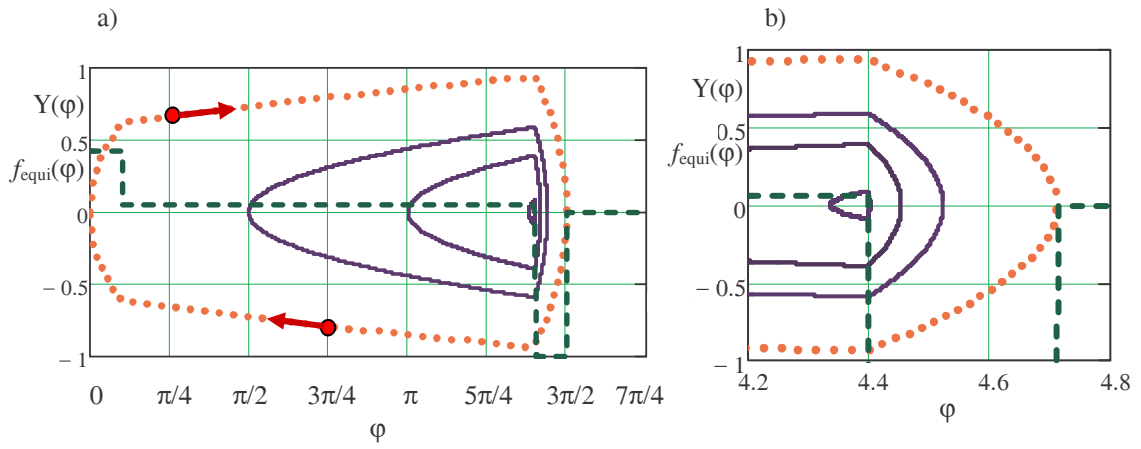
Fig. 12. Particle phase trajectories in the stable phase area (3.4) at acceleration with rectangular barriers calculated with the equations (2.5), (2.6) in Mathcad for $f_{equi}(\varphi)$ (4.7); a) full-sized phase trajectories, b) parts of the trajectories near and inside negative barrier; dot curve is normalized PMS $Y(\varphi)$ (2.4) near separatrix calculated at $\varphi_{inj} = 0.001$, $Y_0 = 0$, arrows indicate momentum shift direction; three solid lines are $Y(\varphi)$ at $\varphi_{inj} = \pi/2$, π and 1.38π, for all three lines $Y_0 = 0$; dashed curve — the barrier function $f_{equi}(\varphi)$ (4.7), $\Delta\varphi_B = \pi/10$, $\Delta\varphi_{BB} = 1.3\pi$

Two examples of particle acceleration above have been considered for idealized parameters when the functions $V_{acc}(\varphi)$ and $V_{dec}(\varphi)$ coincide with absolute precision. In reality some disbalance of these functions exists always, and the integral equalities in (4.5) are violated. It leads to deformation of phase trajectories and their separatrix (Fig. 13). Limitation of disbalance value can be formulated using condition similar to (2.11) and (4.5). In fact, an extreme case takes place when one of the separatrix borders reaches one of the borders of the stable area (3.4). If disbalance exceeds this level particle losses occur at acceleration. The condition of stable acceleration (4.5) can be written now as following:

$$\int_{\varphi_0}^{\varphi_{\max}} f(\varphi) \cdot d\varphi = 0, \quad \text{where}$$

$$\varphi_0 = \begin{cases} \Delta\varphi_B, \\ 0, \end{cases} \quad \varphi_{\max} = \begin{cases} 2\Delta\varphi_B + \Delta\varphi_{BB}, \\ \Delta\varphi_B + \Delta\varphi_{BB}, \end{cases} \quad \text{if} \quad \int_{\Delta\varphi_B}^{\Delta\varphi_B + \Delta\varphi_{BB}} f(\varphi) \cdot d\varphi \Rightarrow \begin{cases} > 0, \\ < 0. \end{cases} \tag{4.9}$$

For instance, in the first example above we find the disbalance restriction

$$\delta f_B \equiv |\Delta f_B + f_{dec}| \leq \frac{\Delta\varphi_B}{\Delta\varphi_{BB} + \Delta\varphi_B}. \tag{4.10}$$

This case is presented in Fig. 13, a. Another case of oscillating disbalance voltage is shown in Fig. 13, b.
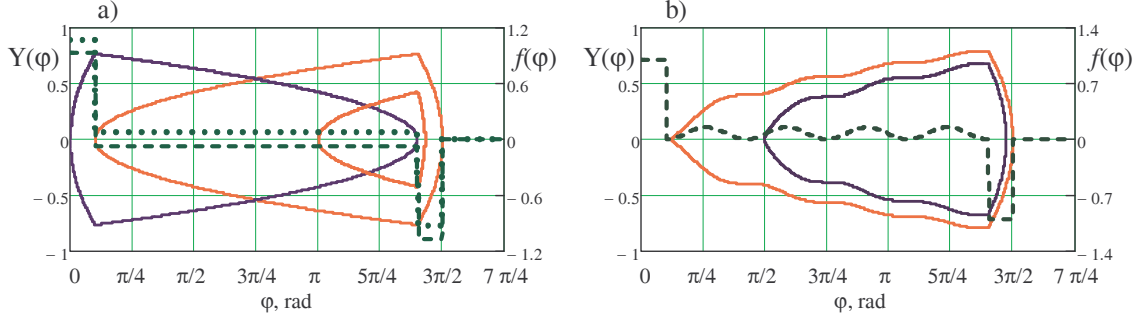
Fig. 13. Influence of disbalance between $V_{acc}(\varphi)$ and $V_{dec}(\varphi)$ functions on particle phase trajectories, the condition (4.10) is met in all cases: a) $\delta f_B(\varphi)$ function is constant in all stable phase area (3.4), $\delta f_B(\varphi) > 0$ — dot line, $\delta f_B(\varphi) < 0$ — dashed line; two right solid curves — separatrix and intermediate phase trajectory at $\delta f_B(\varphi) > 0$, left solid line — separatrix at $\delta f_B(\varphi) < 0$; b) dashed line $\delta f_B(\varphi) = f_d \cdot \left(1 - \cos 8\pi \dfrac{\varphi - \Delta\varphi_B}{\Delta\varphi_{BB}}\right)$, $f_d = \Delta\varphi_B / \Delta\varphi_{BB}$, solid lines — separatrix and an intermediate phase trajectory

One should note that barrier voltage function $f_B(\varphi)$ (and $f_B(\varphi) + \Delta f_B(\varphi)$ in both examples considered in this section does not meet "the no saturation condition" formulated below (see(6.1)). As shown in Section 6, one can remedy this defect rather easily by adding necessary voltage in the injection area.

5. MOVING BARRIERS IN BARRIER BUCKET METHOD

Modern digital electronics allows us manipulating with barrier voltage parameters — amplitude, phase, form and width of voltage pulses in a wide range. A scheme with such parameters is called "moving barrier generator". Application of fast switches

provides control of necessary regimes. Therefore, the simplest version of $f(\varphi)$ function considered in previous sections does not limit all possible schemes used for particle stacking in cyclic accelerators. The most sophisticated schemes with moving barriers have been developed in Fermilab and used for antiproton stacking and beam formation in the rings of the Fermilab accelerator complex [2, 6–9]. Proposed in the 1980th [1] the method of moving barriers has found a new quality when it was supplemented with cooling methods — both stochastic and electron ones.

Here we consider one example of moving barriers scheme that is planed to be used in the NICA collider for ion stacking [13].

The 2π phase space at particle stacking in NICA collider consists of two stable areas $\Delta\varphi_{BB}$ and $\Delta\varphi_{inj}$ divided with two pairs of rectangular barriers as shown in Fig. 14, a; 14, A and described with the following formula:

$$f(\varphi) = \begin{cases} 1, & 0 \le \varphi \le \Delta\varphi_B; & (1) \\ 0, & \Delta\varphi_B < \varphi \le \Delta\varphi_B + \Delta\varphi_{BB}; & (2) \\ -k, & \Delta\varphi_B + \Delta\varphi_{BB} < \varphi \le \varphi_s; & (3) \\ k, & \varphi_s < \varphi \le 3 \cdot \Delta\varphi_B + \Delta\varphi_{BB}; & (4) \\ 0, & 3\Delta\varphi_B + \Delta\varphi_{BB} < \varphi \le 3\Delta\varphi_B + \Delta\varphi_{BB} + \Delta\varphi_{inj}; & (5) \\ 1, & 3\Delta\varphi_B + \Delta\varphi_{BB} + \Delta\varphi_{inj} < \varphi \le 2\pi; & (6) \end{cases} \qquad (5.1)$$

$$0 \le k \le 1.$$

The left stable area $\Delta\varphi_{BB}$ is intended for stack, the right one $\Delta\varphi_{inj}$ — for injected new bunch. They are divided with two barriers of opposite sign and voltage amplitude equal to k (varied further). After new bunch injection into preliminary empty $\Delta\varphi_{inj}$ area both middle barriers are decreased (by modules) synchronously to zero, i. e. $k \to 0$. At certain values of the k the "gate" for injected particles opens and they penetrate from $\Delta\varphi_{inj}$ area into $\Delta\varphi_{BB}$ one (Fig. 14, b; 14, B). At the same time the stack particles are kept in $\Delta\varphi_{BB}$ area. When both barriers decrease even more both bunches merge in a single bunch that occupies the phase area of the size of $\Delta\varphi_{BB} + 2 \cdot \Delta\varphi_B + \Delta\varphi_{inj}$ (Fig. 14, c; 14, C). Generally speaking, the side barriers (equal to unit) can be decreased to zero as well and the merged bunches occupy all circumference of the ring, i.e. phase area of 2π. However, for some technical reasons one could be more preferable to keep the side barriers at constant amplitude.

28
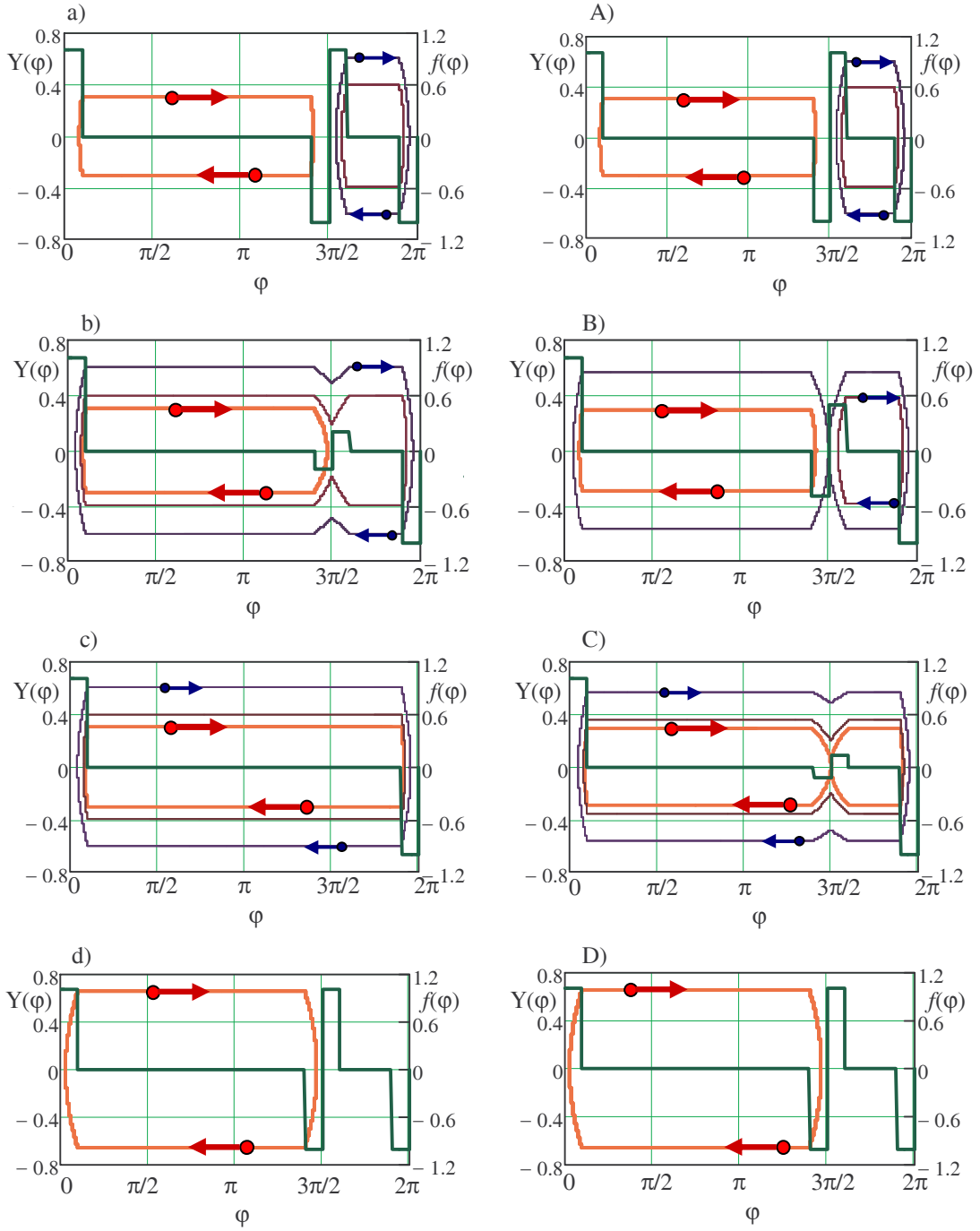
Fig. 14. Dynamics of merging of stacked bunch and injected one: the phase trajectories are numerically calculated with the equations (2.5), (2.6), description in the text, arrows show momentum shift directions. Fast barrier decrease: a) injection of new bunch: $k = 1.0$, $Y_{stack} = 0.3$, $Y_{inj1} = 0.6$, $Y_{inj2} = 0.45$; b) intermediate state "b": $k = 0.2$, $Y_{stack} = 0.3$, $Y_{b1} = Y_{inj1}$, $Y_{b2} = Y_{inj2}$; c) intermediate state "c": $k = 0$, $Y_{stack} = 0.3$, $Y_{c1} = Y_{inj1}$, $Y_{c2} = Y_{inj2}$; d) final state: $k = 1$, $(Y_{stack})_d = 0.702$. Adiabatic barrier decrease: A) injection of new bunch: $k = 1.0$, $Y_{stack} = 0.3$, $Y_{inj1} = 0.6$, $Y_{inj2} = 0.4$; B) intermediate state "B": $k = 0.506$, $Y_{stack} = 0.298$, $Y_{B1} = 0.564$, $Y_{B2} = 0.385$; C) intermediate state "C": $k = 0.288$, $Y_{stack} = (Y_{stack})_{penetration} = 0.288$, $Y_{C1} = Y_{B1}$, $Y_{C2} = (Y_2)_{penetration} = 0.352$; D) final state: $k = 1$, $(Y_{stack})_D = 0.661$

29

The next step consists of adiabatic displacement of right side negative barrier into position of former middle negative barrier and restoration of all four barriers into initial positions. As result the stack is compressed in phase and increased in momentum spread (Fig. 14, d; 14, D).

The barriers decrease has two outmost regimes: the *fast* and the *adiabatic* ones, i. e. varied during time much shorter (fast) or much longer (adiabatic) than the periods of particle traveling along phase trajectory — both for stack particles and for injected ones (see (1.12) and (2.21)).

5.1. Fast barrier decrease

At fast ("instant"!) barrier decrease a particle continues its phase motion along phase trajectory that is defined with particle trajectory parameters at the moment of barrier switching OFF, i. e. having certain Y_{switch} momentum and φ_s with phase. It means the outer trajectory of injected particles (thin outer curve in Fig. 14, b) and merged bunches (thin outer curve in Fig. 14, c) are defined with $Y_{switch} = Y_{inj1}$ (Fig. 14, a). Thus, the bunch emittance ε_c in Fig.14, c is described with Formula (2.19) at $Y_{max} = Y_{inj1}$. Then, after merged bunches *adiabatic compression*, the Y_{fnl} value on the outer phase trajectory is defined again with equation (2.19) where $\varepsilon(Y_{max}) = \varepsilon_c$ is emittance of the merged bunch before compression. To find Y_{fnl} value we have to solve now the cubic equation (2.19). It can be done numerically, as we had to do for finding parameters of trajectories in Fig. 14 and have found by such a method $(Y_{stack})_d$ equal to 0.702 (Fig. 14, a–d).

5.2. Adiabatic barrier decrease

Before detailed description of the regime of adiabatic barriers decrease we need to make some additional examination of particle dynamics in the *RF system with different heights of the voltage barriers*. And this examination we begin with $\Delta\varphi_{inj}$ area (Fig. 15). Executing calculations similar to (2.14)–(2.19) for *rectangular barriers* one can obtain the following results for phase trajectory parameters in the *injection area* $\Delta\varphi_{inj}$:

$$Y_{\text{inj}}(\varphi) = \begin{cases} \sqrt{2k(\varphi - \varphi_{\min})}, & \varphi_{\min} \le \varphi \le 3\Delta\varphi_B + \Delta\varphi_{BB}, \\ \sqrt{2k \cdot \Delta\varphi_0} \equiv Y, & 3\Delta\varphi_B + \Delta\varphi_{BB} \le \varphi \le 3\Delta\varphi_B + \Delta\varphi_{BB} + \Delta\varphi_{\text{inj}}, \\ \sqrt{2k(\varphi_{\max} - \varphi)}, & 3\Delta\varphi_B + \Delta\varphi_{BB} + \Delta\varphi_{\text{inj}} \le \varphi \le 2\pi - \Delta\varphi. \end{cases} \quad (5.2)$$

Here (see symbols in Fig. 16)

$$\varphi_{\min} = 3\Delta\varphi_B + \Delta\varphi_{BB} - \Delta\varphi_0, \quad \varphi_{\max} = 2\pi - \Delta\varphi. \quad (5.3)$$

We can write also two evident equalities. The first one follows from the condition

$$\int_{\varphi_{\min}}^{3\Delta\varphi_B + \Delta\varphi_{BB}} f(\varphi) \cdot d\varphi = \int_{\varphi_{\max} - \Delta\varphi}^{\varphi_{\max}} f(\varphi) \cdot d\varphi.$$

It gives

$$k \cdot \Delta\varphi_0 = \Delta\varphi. \quad (5.4)$$

The second one is the condition of particle penetration from injection area into the stack one:

$$\Delta\varphi_0 = \Delta\varphi_B. \quad (5.5)$$

At this condition we find from (5.2) the value of particle momentum at beginning of its penetration in the stack area:

$$Y_{penetration} = \sqrt{2k \cdot \Delta\varphi_B}. \quad (5.6)$$

Later on we need Formulae for bunch emittance of particles kept between two barriers of different heights. Performing calculations similarly to (2.18), (2.19) with the expression (5.2) for $Y_{\text{inj}}(\varphi)$ we obtain Formulae for *injected bunch emittance*:

$$\varepsilon_{\text{inj}}(k) = \sqrt{2k} \left[\frac{4}{3} \cdot (1+k) \cdot \Delta\varphi_0^{3/2} + 2 \cdot \sqrt{\Delta\varphi_0} \cdot \Delta\varphi_{\text{inj}} \right] = \frac{2}{3} \cdot \frac{1+k}{k} \cdot Y^3 + 2 \cdot Y \cdot \Delta\varphi_{\text{inj}}. \quad (5.7)$$

Here Y is the Y_{inj} value between the barriers (see (5.2)).

Expressions for $Y_{stack}(\varphi)$ (*stack area*) and emittance of stack bunch ε_{stack} can be obtained similarly. For stack emittance one has to replace in (5.7) $\Delta\varphi_{\text{inj}}$ with $\Delta\varphi_{BB}$. Then we find

$$Y_{stack}(\varphi) = \begin{cases} \sqrt{2k(\varphi - \varphi_{\min})}, & (\varphi_{stack})_{\min} \le \varphi \le \Delta\varphi_B, \\ \sqrt{2k \cdot \Delta\varphi_{stack1}} \equiv Y, & \Delta\varphi_B \le \varphi \le \Delta\varphi_B + \Delta\varphi_{BB}, \\ \sqrt{2k(\varphi_{\max} - \varphi)}, & \Delta\varphi_B + \Delta\varphi_{BB} \le \varphi \le \Delta\varphi_B + \Delta\varphi_{BB} + (\varphi_{stack})_{\max}, \end{cases} \quad (5.8)$$

$$(\varphi_{\min})_{stack} = \Delta\varphi_B - \Delta\varphi_{stack1}, \quad (\varphi_{\max})_{stack} = \Delta\varphi_B + \Delta\varphi_{BB} + \Delta\varphi_{stack2}.$$

31

$$\varepsilon_{stack}(k) = \sqrt{2k}\left[\frac{4}{3}\cdot(1+k)\cdot\Delta\varphi_0^{3/2} + 2\cdot\sqrt{\Delta\varphi_0}\cdot\Delta\varphi_{BB}\right] = \frac{2}{3}\cdot\frac{1+k}{k}\cdot Y^3 + 2\cdot Y\cdot\Delta\varphi_{BB}. \quad (5.9)$$

Symbol Y here is defined in second line of the expression (5.8) for $Y_{stack}(\varphi)$. Symbol $\Delta\varphi_{stack2}$ is shown in Fig. 15, $\Delta\varphi_{stack1}$ has similar meaning for stack particle trajectory in first $\Delta\varphi_B$ area. Evidently, instead equalities (5.4), (5.5) we can write

$$\Delta\varphi_{stack1} = k\cdot\Delta\varphi_{stack2}, \quad \Delta\varphi_{stack2} = \Delta\varphi_B. \quad (5.10)$$
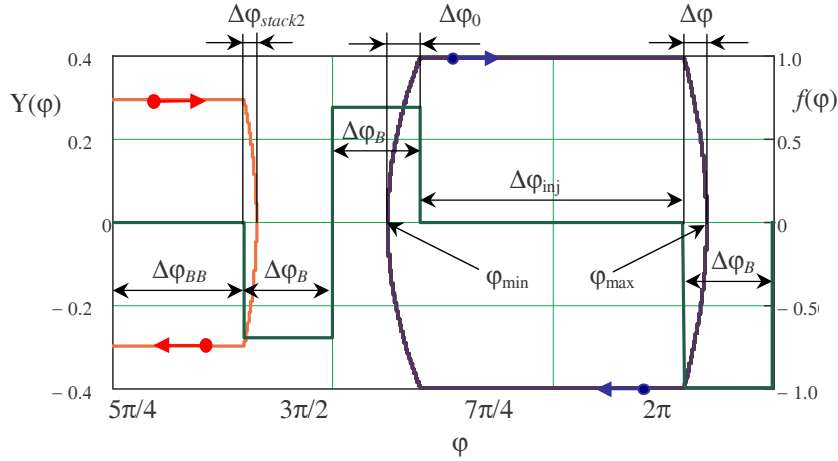
Fig. 15. Particle trajectories in the stack phase area (left curve) and in the injection one (right curve); the stack particle trajectory is shown in part; the barriers have equal phase spans and the following amplitudes: $V = -V_4 = 1$, $V_2 = -V_3 = -0.4$, $\Delta\varphi_B = \pi/10$, $\Delta\varphi_{BB} = 1.3\cdot\pi$; the phase trajectories are numerically calculated with the equations (2.5), (2.6), description in the text, arrows show momentum shift directions

Now we are ready for description of particle phase dynamics at *adiabatic barrier decrease* (Fig. 14, A–D). The procedure of calculation of particle trajectory parameters we begin with

Stage A (Fig. 14, A). For given initial Y — values of 3 trajectories, i. e. Y_{stack}, Y_{inj1} and Y_{inj2}, we calculate the values of phase trajectory areas ("emittances") with second expression in the Formulae (5.7) and (5.9): ε_{stack}, ε_{inj1}, ε_{inj2}.

Stage B (Fig. 14, B) — beginning of particles Y_{inj1} penetration into stack area. First of all, one should consider deformation of the phase trajectory during decrease of the middle barriers. This process is accompanied with expansion of the trajectories along abscissa in Fig. 15 that leads to displacement of the points φ_{min} and φ_{max} to the left and to the right correspondingly. Due to phase space area conservation (adiabatic invariant!) it compresses along ordinate axis leading to decrease of Y values. When φ_{min}

and φ_{max} points reach the outer borders of the barriers (i. e. the condition (5.5) is met) the particle penetration into adjacent area begins.

Now we need to find a value of k_B corresponding to this stage. It has to be done by solving of cubic equation for k_B (first expression in (5.7)) at given ε_{inj1} and $\Delta\varphi_0 = \Delta\varphi_B$. Then from (5.6) at $k = k_B$ we find the value of Y_{B1}. To find the values of Y_{stack} and Y_{B2} we solve the cubic equations for Y (second expressions in (5.7) and (5.9)) at $k = k_B$ and corresponding values of emittances ε_{inj2} and ε_{stack}.

Stage C (Fig. 14, C) — beginning of stack particles penetration into injection area. The calculation procedure is similar to that one at stage B: finding k_C and the values of all three Y-parameters. All three phase trajectories merge together occupying both stack and injection areas.

One should underline that all three emittances, ε_{stack}, ε_{inj1} and ε_{inj2}, do not remain constant, but increase after penetration in the adjacent area at the stages B and C, because particles when penetrated move freely in phase space with negligibly week interaction with decreasing middle barriers. As result, the Y values of these particles do not change during the barriers decrease further to zero. E. g., for this reason at the beginning of stack particle penetration in the injection area (stage C) we have $Y_{stack} = (Y_{stack})_{penetration} = 0.288$, $Y_{C1} = Y_{B1}$, $Y_{C2} = (Y_2)_{penetration} = 0.352$. The last Y-parameter reaches the shown value at $k = 0.197$ and keeps it further.

Stage D (Fig. 14, D) — adiabatic compression of all particles. The final size of compressed bunch we find from condition of outer phase trajectory area conservation: $(Y_{stack})_D = 0.661$. This value is slightly less of $(Y_{stack})_d = 0.702$ obtained at fast decrease of the middle barriers. Such a small difference is result of chosen small width of the barriers when contribution of the middle barrier area is rather insignificant.

Similar procedure is explained in the Ref. 2 on the language of energy variation. By our opinion that conceals the picture of particle dynamics in phase space.

In the case of cooling application the described scheme with moving barriers has significant advantage comparatively to that one considered in section 3. It moderates essentially requirement to cooling time (3.6), (3.7). Indeed, one has to cool down new injected particles only to the level when their maximum PMS at the stages "b" and "B"

(Fig. 14) is less than Y_{sep} in $\Delta\varphi_{BB}$ area. After merging of injected bunch and stack and forming final stages "d" or "D" one can continue cooling having more time for this purpose.

Another advantage of this scheme shows up at cooling also. In the case of stochastic cooling application we have a significant gain in cooling rate when bunches are merged and occupy all circumference of the ring. The cooling rate is inversely proportional to linear density of particles, therefore the gain factor is of the order of $2\pi/\Delta\varphi_{inj}$ [17]. For electron cooling the gain is not so evident. Nevertheless, reduction of linear density of stored beam is preferable to reduce effects of beam space charge.

6. BARRIER RF VOLTAGE TECHNIQUE

Modern barrier RF systems are constructed with digitally controlled driving generators and power amplifiers having solid-state voltage switches. Such a device is able to produce short high voltage pulses of rectangular form with steep edges and minimal ripple amplitude. The device feeds an RF cavity loaded with ferromagnetic (ferrite, amorphous iron, etc.).

The ferromagnetic load leads to some peculiarity of barrier RF systems: the voltage function $f(\varphi)$ has to meet "the no saturation condition":

$$\int_0^{2\pi} f(\varphi)\cdot d\varphi = 0. \tag{6.1}$$

If not the ferromagnetic will be saturated after certain number (not so big!) of barrier voltage pulses (magnetic flux is proportional to time integral of the $V(t)$ function).

The barrier RF systems have typically frequency bandwidth in the range of tens of kHz to hundreds of MHz.

Most sophisticated barrier RF systems were developed in Fermilab since first pioneering works fulfilled there (Table 1).

34

Table 1. Parameters of barrier RF systems at Fermilab accelerator facility [2]

Accelerator/Storage ring & Function of Barrier RF System	Ferrite Type (Cavity Dimension)	Properties: Power, V_{peak}, R_{shunt}, Bandwidth, Power Amplifiers
Debuncher – Gap preserving	MnZn + NiZn (~ 1 m)	2.4kW, 700V, 104 Ω, 10kHz−10MHz, IFI3100S
Accumulator – Ion clearing and isolated bucket	MnZn + NiZn (~ 1 m)	100W, 70V, 50 Ω, 10kHz−10MHz, ENI2100
Recycler – for all RF manipulations	Ceramic Magnetics MN60, CMD10 (~1 m)	4×3.5kW, 4×500V, 4×50Ω, 10kHz−100MHz, Amplifier Research, Model 3500A100
MI –Test cavity	FinemetRcore (~0.75 m)	150kW, 10kV, 500Ω, Fast Switch
MI – Damper Cavities	MnZn + NiZn (~1 meter)	3×3.5kW, 3×500V, 3×50Ω, 10kHz−100MHz, Amplifier Research, Model 3500A100

Parameters of some barrier RF systems developed in recent years and under development are presented in Table 2.

Table 2. Parameters of some barrier RF systems

Laboratory (accelerator) / Parameter	BNL/KEK (AGS) [18]	KEK for BNL (AGS) [19]	Budker INP for JINR (NICA Collider) [20]
Core material	ferrite	Finemet[*]	amorphous iron
Gaps per cavity	4	4	14
f_{res}, MHz	2.6	1.1	0.579÷0.587
R/Q per gap, Ohm	180	1500	—
Q	30	0.6	—
Amplifier rating, kW	600	120	22

[*] Trademark, Hitachi Metals, Ltd.

Barrier RF systems become more and more popular in accelerator technologies as solid-state powerful RF electronics is getting growing improvements.

CONCLUSION

Application of Barrier Bucket RF system to storage and acceleration charged particles in synchrotrons and storage rings has significant advantages in comparison with classic RF harmonic systems. Especially it becomes apparent when one deals with heavy particles like protons and ions where using of cooling methods is unavoidable practically.

The technique of BB method well developed since its first proposal and allows presently to construct very sophisticated RF schemes using potentials of modern solid-state electronics.

The method of analysis charge particle dynamics in BB Systems presented here allows to perform rather easily analytical calculations of the system parameters and obtain a complete description of particle dynamics characteristics in a wide parameter range. Supplemented with numerical simulations such an approach guarantees a proper choice of parameters of the BB system when it is under design.

This method can be applied efficiently to analysis of particle dynamics with harmonic RF systems.

ACKNOWLEDGEMENTS

REFERENCES

1. J. E. Griffin et al., IEEE, Trans. Nucl. Sci., NS-30, 3502 (1983).

2. C. M. Bhat, Applications of barrier bucket RF systems at Fermilab, Fermilab-Conf-06-102-AD, 2006.

3. I. Meshkov, V. Kekelidze, R. Lednicky, V. Matveev, A. Sorin, G. Trubnikov, NICA project at JINR, Proc. of COOL'2011 Workshop, MOIO02, http://accelconf.web.cern.ch/accelconf/, 2011.

4. M. Steck, The FAIR Accelerator Facility, Proc. of STORI'2008.

5. A. Kolomensky and A. Lebedev, Theory of cyclic accelerators, FizMatLit, Moscow, 1962 (in Russian), translated into English: Springer, N.-H., Amsterdam, 1966.

6. C. M. Bhat, Antiproton stacking and un-stacking in the Fermilab recycler ring, Proc. of PAC'03, WPPE010, http://accelconf.web.cern.ch/accelconf/, 2003.

7. C. M. Bhat, Barrier RF systems in synchrotrons, Proc. of EPAC'2004, THOBCH03, http://accelconf.web.cern.ch/accelconf/, 2004.

8. G. W. Foster, C. M. Bhat, B. Chase, K. Seiya, J. A. MacLachlan, P. Varghese, D. Wildman, Beam manipulation and compression using broad band RF systems in the FERMILAB Main Injector and Recycler, ibid, TUPLT149.

9. C. M. Bhat, A new technique for making bright proton bunches using barrier FR systems, Proc. of PAC'05, TPAP021, http://accelconf.web.cern.ch/accelconf/, 2005.

10. M. Steck, D. Krestnikov, I. Meshkov, R. Pivin, A. Sidorin, A. Smirnov, C. Dimopoulou, G. Schreiber, Particle article accumulation using barrier bucket RF system, Proc. of COOL'09, TUM2MCIO02, http://accelconf.web.cern.ch/accelconf/, 2009.

11. T. Katayama, C. Dimopoulou, F. Nolden, G. Schreiber, M. Steck, H. Stockhorst, T. Kikuchi, Simulation study of barrier bucket accumulation with stochastic cooling at GSI ESR, Proc. of COOL'11, TUPS19, http://accelconf.web.cern.ch/accelconf/, 2011.

12. T. Katayama, I. Meshkov and G. Trubnikov, Numerical investigation of stochastic cooling at NICA collider, Ibid, TUIOB01

13. A. V. Eliseev, O. S. Kozlov, I. N. Meshkov, A. O. Sidorin, A. V. Smirnov, G. V. Trubnikov, T. Katayama, V. N. Volkov, E. K. Kenzhebulatov, G. Y. Kurkin, V. M. Petrov, Storage acceleration and short bunched beam formation of 197AU+79 ions in the NICA collider, Ibid, MOBCH01.

14. M. Steck, C. Dimopoulou, B. Franzke, O. Gorda, T. Katayama, F. Nolden, G. Schreiber, D. Moehl, R. Stassen, H. Stockhorst, I. Meshkov, A. Sidorin, G. Trubnikov, Demonstration of longitudinal stacking in the ESR with barrier buckets and stochastic cooling, TUPS20, Proc. of COOL'11, http://accelconf.web.cern.ch/accelconf/, 2011.

15. T. Bohl, T. Linnecar, E. Shaposhnikova, Barrier buckets in the CERN SPS, Proc. of EPAC'00, THP2A10, http://accelconf.web.cern.ch/accelconf/, 2000.

16. A. V. Smirnov, private communication (2012).

17. D. Moehl, Stochastic Cooling, Proceedings of CERN Accelerator School CAS-1985, CERN, 1987, pp. 453–520.

18. M. Blaskiewicz, J. M. Brennan, T. Roser, K. Smith, R. Spitz, A. Zaltsman, BNL, M. Fujieda, Y. Iwashita, A. Noda, Kyoto University, Gokanosho, M. Yoshii, Y. Mori, C. Ohmori, Y. Sato, Barrier cavities in the Brookhaven AGS, Proc. of PAC'99, WEP10, http://accelconf.web.cern.ch/accelconf/, 1999.

19. M. Fujieda, Y. Iwashita and A. Noda, Y. Mori, C. Ohmori, Y. Sato, M. Yoshii, M. Blaskiewicz, J. M. Brennan, T. Roser, K. S. Smith, R. Spitz, A. Zaltsmann, Magnetic alloy loaded RF cavity for barrier bucket experiment at the AGS, Proc. of PAC'99, MOP81, http://accelconf.web.cern.ch/accelconf/, 1999.

20. G. Ya. Kurkin, V. M. Petrov et al., Conceptual design report of acceleration RF systems of NICA collider, Budker INP, July 2012.

Отпечатано методом прямого репродуцирования
с авторского оригинала.